Katalin Luca Komporday

Development of IL-11 receptor targeting miniproteins

Master of Biotechnology

Supervisors:

Gabor Oroszlan PhD

Co-supervisor

Professor Deborah Mary Power

UNIVERSIDADE DO ALGARVE

Faculty of Science and Technology

2025

Development of IL-11 receptor targeting miniproteins

MASTER IN BIOTECHNOLOGY

AUTHORSHIP STATEMENT

I declare I am the author of this work, which is original and unpublished. The sources consulted have been duly cited in the text and included in the list of references.

Katalin Luca Komporday

Acknowledgement

I would like to express my sincere gratitude to everyone who supported me during my master's thesis journey. First, I am grateful to my supervisor, Gábor Oroszlán, PhD, for his guidance, support, and insightful feedback. I also sincerely thank my academic supervisor, Professor Deborah Mary Power, PhD, for her guidance and support throughout the master's program. I appreciate VRG Therapeutics Zrt. for the opportunity to conduct my master's thesis research in their laboratory and contribute to their project. I particularly thank Mariann Kremlitzka, PhD, and József Murányi, PhD, for their significant contributions to the mammalian expression of the IL-11 cytokine and the purification of proteins and peptide preparation, respectively. I especially value the support and mentorship of Ambrus Gordos, Kremlitzka Mariann, PhD, and the entire team. I would like to thank Csilla Masa for her assistance and encouragement during the experimental work. Their willingness to share their expertise greatly contributed to the successful completion of this laboratory work and my master's thesis. I also thank the faculty and academic staff of the Biotechnology Master's program at the University of Algarve for their academic support, as well as my colleagues and friends for their help and motivation throughout this journey. Finally, I am deeply grateful to my family for their constant support, encouragement, and patience, which gave me the strength and motivation to complete this thesis.

Abstract

De novo protein design has emerged as a transformative approach for creating novel therapeutic molecules with highly specific functions and tailored structures. This thesis presents the design and development of miniproteins targeting the interleukin-11 receptor alpha (IL-11Rα), a key mediator in fibrotic diseases such as idiopathic pulmonary fibrosis (IPF). Miniproteins, small stable peptides with well-defined tertiary structures, offer advantages over traditional therapies by small molecules or antibodies through higher selectivity, improved tissue penetration, and lower risk of immunogenicity. Leveraging AI-driven bioinformatics tools, a library of 400 different miniprotein scaffolds was designed to selectively bind the IL-11Rα, competing with its natural ligand, IL-11 cytokine. The miniprotein library was synthesized as an oligonucleotide pool, cloned into phagemid vectors, and expressed on the pIII M13 bacteriophage surface for phage display-based selection. A biopanning campaign was used to enrich miniproteins with strong binding affinities for IL-11Rα across multiple screening rounds. Two lead candidates, DN226 and DN213 demonstrated high specificity and affinity confirmed by ELISA assays. However, DN226 showed a better affinity and competitiveness against the IL-11 cytokine for binding to the receptor compared to DN213. Since transient transfection expression of IL-11Rα in FreeStyle Human Embryonic Kidney (HEK293-F) cells faced yield and aggregation challenges, commercially sourced IL-11Rα was employed in downstream assays. The combination of computational design with classical biotechnological approaches enabled the rapid identification of functional miniproteins capable of binding the IL-11Rα. This work underscores the potential of AI-driven de novo protein design as a versatile technology for precise drug discovery and development. The identified miniproteins provide promising hit molecules for developing innovative, targeted anti-fibrotic therapies. Future work should focus on optimizing miniprotein candidates and evaluating their efficacy in cell-based and in vivo studies, paving the way for novel treatment approaches for fibrotic diseases, like IPF.

Sumário

O design de proteínas *de novo* surgiu como uma das fronteiras mais poderosas da biotecnologia moderna, permitindo a criação de biomoléculas completamente novas com estruturas e funções biológicas altamente específicas. Esta abordagem transformacional é especialmente atraente para doenças nas quais as terapias convencionais, como anticorpos monoclonais ou pequenas moléculas, têm demonstrado baixa eficácia ou pouca acessibilidade aos tecidos. As doenças fibróticas, incluindo a fibrose pulmonar idiopática (FPI), representam uma área de grande necessidade médica, na qual estratégias moleculares inovadoras são urgentemente necessárias. Na última década, a citocina interleucina-11 (IL-11) ganhou reconhecimento como um fator central da fibrose em vários órgãos. A IL-11 promove a ativação de fibroblastos, a transformação em miofibroblastos, a deposição excessiva de colagénio e a remodelação desregulada dos tecidos, principalmente através de vias dependentes de ERK. O alvo do eixo IL-11/receptor alfa da IL-11 (IL-11Rα) surgiu, portanto, como uma estratégia terapêutica promissora, oferecendo a perspectiva de interromper ou mesmo reverter os processos fibrogénicos na sua origem molecular. A FPI é caracterizada por cicatrizes crónicas e progressivas do parênquima pulmonar, com perda de elasticidade pulmonar, comprometimento da troca gasosa, falta de ar e, por fim, insuficiência respiratória. Apesar dos avanços significativos na compreensão da sua fisiopatologia, a FPI continua a ser uma doença fatal, com uma sobrevivência média de apenas 2 a 3 anos após o diagnóstico. A pirfenidona e o nintedanibe são medicamentos antifibróticos atualmente aprovados que podem retardar a progressão da doença, mas não revertem a fibrose estabelecida; ambos estão associados a efeitos adversos substanciais. Portanto, o desenvolvimento de terapêuticas que intervenham a montante na cascata fibrogênica é fundamental para melhorar os resultados dos pacientes.Neste contexto, as miniproteínas representam uma nova classe de moléculas especialmente adequadas para atingir interações proteína-proteína extracelulares. Concebidas para variar entre 1 e 10 kDa, as miniproteínas têm arquiteturas compactas estabilizadas por núcleos hidrofóbicos, elementos de estrutura secundária e comportamento de dobragem cooperativa. O seu tamanho reduzido permite uma penetração nos tecidos superior em comparação com os anticorpos, enquanto as superfícies concebidas computacionalmente permitem uma ligação de alta afinidade e alta especificidade a alvos terapêuticos. Esses avanços são agora aprimorados pela rápida geração de diversas estruturas de miniproteínas com precisão atómica por meio de plataformas de previsão estrutural baseadas em aprendizado de máquina, como RFdiffusion, ProteinMPNN e AlphaFold2. Essas ferramentas, por sua vez, combinadas com métodos de seleção empíricos, estabelecem uma estrutura sólida para a descoberta de novas terapias que atuam contra alvos moleculares desafiadores, como o IL-11Rα.

Com base nesses avanços, este trabalho concentrou-se no design de novo de miniproteínas que se ligam ao IL-11Rα e inibem competitivamente a sua interação com o IL-11. Um total de 400 miniproteínas estruturalmente diversas foram projetadas computacionalmente usando pipelines assistidos por IA otimizados tanto para complementaridade de forma quanto para afinidade de ligação prevista. As sequências projetadas foram sintetizadas como um conjunto de oligonucleotídeos e clonadas no fagémido pAS62 para exibição monovalente na proteína pIII do bacteriófago M13. Esse formato permitiu a triagem simultânea de centenas de candidatos por meio de uma campanha iterativa de seleção de exibição de fagos. Abordagens paralelas incluíram a expressão de IL-11Rα recombinante em células FreeStyle HEK293-F de mamíferos para permitir a produção de um recetor biologicamente relevante para ensaios de ligação. A expressão e purificação de IL-11Rα interna foram dificultadas

devido aos baixos rendimentos e à agregação de proteínas durante o processamento a jusante. Para garantir condições de seleção confiáveis e reproduzíveis, o IL-11Rα obtido comercialmente foi usado nas etapas subsequentes de triagem e validação. A biopanning com exibição de fagos foi realizada utilizando IL-11Rα imobilizado como alvo num processo de enriquecimento seletivo de quatro rondas. Cada etapa aumentou o rigor das condições de lavagem para o isolamento de miniproteínas com atividade de ligação válida e de alta afinidade. Os clones de fagos individuais, obtidos após a última etapa de enriquecimento, foram selecionados através de ELISA para a sua interação com IL-11Rα e para o seu potencial de competir eficazmente com IL-11 na ligação ao recetor. Deste processo de seleção e triagem surgiram dois candidatos principais, nomeadamente DN226 e DN213. Estas duas miniproteínas demonstraram uma elevada ligação específica ao IL-11Rα, que foi validada quantitativamente através de ensaios ELISA. Significativamente, estes ensaios competitivos demonstraram a capacidade de ambos os candidatos inibirem a ligação da IL-11 ao seu recetor, destacando as suas capacidades em interromper o complexo IL-11/IL-11Rα/gp130 que é formado para sinalização. Destes, o DN226 exibiu afinidade superior, maior inibição competitiva contra a IL-11 e, em geral, um comportamento molecular mais promissor, identificando-o como a molécula mais adequada para desenvolvimento pré-clínico adicional.

Este trabalho serve para destacar uma abordagem eficaz e robusta que permite a integração do design computacional de novo de proteínas com técnicas de seleção experimental no desenvolvimento de miniproteínas terapêuticas direcionadas a vias relevantes para doenças. Os resultados ilustram a capacidade de pequenas proteínas projetadas computacionalmente de reconhecer seletivamente um receptor de citocina complexo e interferir na sua interação com o ligante, representando uma nova geração de agentes antifibróticos. O estudo representa ainda uma valiosa prova de conceito de que a via de sinalização da IL-11, há muito implicada na progressão fibrótica, pode ser modulada com precisão através de estruturas proteicas racionalmente concebidas, em vez de grandes produtos biológicos. As direções futuras devem incluir um maior refinamento estrutural do DN226 para aumentar a estabilidade, a afinidade e a meia-vida sérica; validação funcional em modelos de fibroblastos e células epiteliais pulmonares; e avaliação em modelos animais de fibrose pulmonar para determinar a eficácia terapêutica in vivo. Além disso, estratégias de otimização como PEGilação, fusão Fc ou ciclização podem melhorar ainda mais as propriedades farmacocinéticas, apoiando o eventual desenvolvimento translacional. Em suma, as miniproteínas aqui descritas constituem uma base muito promissora para uma nova classe de terapêuticas antifibróticas direcionadas para o IL-11Rα. A sinergia atual entre o design biomolecular baseado em IA e as metodologias laboratoriais clássicas sublinha a viabilidade e o poder de tal abordagem para combater doenças complexas como a FPI.Com os avanços contínuos na tecnologia computacional, proteínas projetadas de novo, como a DN226, podem abrir caminho para terapias cada vez mais precisas, eficazes e acessíveis para doenças fibróticas e outras condições.

Table of Contents

List of abbreviations

BSA: Bovine serum albumin

CHR: Cytokine-binding homology region

DPBS: Dulbecco's phosphate-buffered saline

ECM: Extracellular matrix

ELISA: Enzyme-linked Immunosorbent Assay

EMT: Epithelial-mesenchymal transition

ERK: Extracellular signal-regulated kinase 1/2

Gp130: Glycoprotein 130 kDa

HEK293-F: FreeStyle human embryonic kidney 293-cells

HRP: Horseradish peroxidase

IL-11: Interleukin-11

IL-6: Interleukin-6

IL-11Rα: Interleukin-11 receptor alpha

cIL-11Rα: Commercially available interleukin-11 receptor alpha

rIL-11Rα: Recombinant interleukin-11 receptor alpha (in-house)

sIL-11Rα: Soluble interleukin-11 receptor alpha

IL-6Rα: Interleukin-6 receptor alpha

sIL-6Rα: Soluble interleukin-6 receptor alpha

IPF: Idiopathic pulmonary fibrosis

JAK: Janus Kinase

Kd: Dissociation constant

Ki: Inhibitory constant

LB medium: Luria-Bertani medium

MAPK: Mitogen-activated protein kinase

PBS: Phosphate-buffered saline

PCR: Polymerase chain reaction

RFdiffusion: Rosetta Folding Diffusion

SDS-PAGE: Sodium dodecyl sulfate polyacrylamide gel electrophoresis

STAT: Signal transducer and activator of transcription

TGF-ß: Transforming growth factor bet

1 General Introduction- State of the Art

Signal pathways are the foundation of internal communication and responses to the external environment, enabling various cell types to coordinate their actions through cell-cell communication. Many distinct signaling pathways have been developed for effective cell communication, ensuring normal development, homeostasis, and host defense (Su et al., 2024). Cells use this complex communication to sense their environment, process signals, and respond to various stimuli. Many different signals can trigger signaling pathways, including a large group of molecules known as cytokines (Iqbal et al., 2010). Each cytokine can exert unique biological activities due to different expression patterns and binding affinities for signaling molecules of cytokine receptors (Hirano et al., 1997). Interestingly, these signaling mechanisms are cell-specific, as one cytokine can express different biological activities on different target cells (Hirano et al., 1997; Tenney et al., 2005). This feature can be attributed to several reasons. For instance, different signaling pathways can be activated on different targets through the same co-receptor, like the signal-transducer glycoprotein 130 kDa (gp130) receptor. It is due to the different responses of cells to the different gp130 stimulations and the differences in the final transcriptional activation of target genes. In addition, the interplay and balance between the intracellular signaling pathways could define the outcome of the signal transduction as well (Hirano et al., 1997).

1.2 Overview of Cytokine Signaling

Cytokines are small (15-20 kDa), short-lived soluble proteins produced by various cell types, such as lymphocytes, macrophages, and natural killer cells (NK cells) (Liu et al., 2021; Rose-John, 2018). They regulate different biological functions, both immunological and non-immunological, and are key signaling molecules in cell interactions and communications (Curfs et al., 1997; Zhang & An, 2007).

Various cells often produce the same cytokine, and a single cytokine can affect multiple cell types (known as pleiotropy). They are frequently made in cascades and can work synergistically or antagonistically to regulate responses (Zhang & An, 2007). Cytokines can bind to their receptors on the cell that produced them (autocrine signaling), on nearby cells (paracrine signaling), or, in some cases, they can act on distant cells

(endocrine signaling) (Leonard & Lin, 2000; Zhang & An, 2007). Interaction with their receptors initiates a cascade of intracellular signaling through different signaling pathways, leading to the expression of the target gene and a biological response (Dinarello, 2007; Kaminska, 2005). They influence many mechanisms, including innate and adaptive immune response, inflammation, disease pathogenesis, embryonic development, changes in cognitive function, and aging (Dinarello, 2007; Goodman et al., 2003; Kany et al., 2019; Medzhitov & Janeway, 1997). Thus, cytokine levels can serve as essential indicators for clinical disorders, as altered or increased levels of these molecules can lead to organ failure or even death (Liu et al., 2021).

Categorizing cytokines has become challenging due to their secretion by various cell types and diverse biological properties. Consequently, "cytokine" serves as a general term, encompassing a superfamily that includes several groups, including interleukins (ILs), interferons (IFNs), chemokines, and numerous other mediators (Dinarello, 2007). This thesis focuses solely on the interleukin-6 family, with a particular emphasis on interleukin-11.

1.3 Signaling of Interleukin-11

Interleukin-11 (IL-11) is a member of the interleukin-6 family, along with interleukin-6 (IL-6), ciliary neurotrophic factor (CNTF), leukemia inhibitory factor (LIF), oncostatin M (OSM), cardiotrophin 1 (CT-1), cardiotrophin-like cytokine (CLC), and IL-27 (Rose-John, 2018). On one hand, they have an essential role in physiological mechanisms in the nervous, endocrine, and cardiovascular systems, in inflammation, acute phase reaction, and are key players in immune responses (Heinrich et al., 2003; Hirano et al., 1997). On the other hand, IL-6 family cytokines have been linked with the onset and maintenance of different diseases, including fibrotic diseases, rheumatoid arthritis, nonalcoholic fatty liver disease, and cancer (Ayaub et al., 2017; Dayer & Choy, 2010; Fearon et al., 2006; Kumari et al., 2016; Schafer et al., 2017; Widjaja et al., 2019).

The IL-6-type cytokines exert their effects through signal transducers and coreceptors, activating signaling pathways such as the MAPK and JAK/STAT (Janus kinase/signal transducer and activator of transcription) cascades (Heinrich et al., 2003). The membrane-bound signal transducer, gp130, is expressed in all cells of humans; however, these receptors need an additional interleukin subunit to activate the signaling

(through gp130) (Reeh et al., 2019; Rose-John, 2018). The gp130 receptor is referred to as the ß-subunit, while the cytokine-specific subunit, which binds the ligand, is the α-subunit (such as IL11-R) (Tenney et al., 2005). After the IL-11 receptor (IL11-Rα) binds IL-11, the IL11/IL11Rα complex associates with gp130, which then homodimerizes, leading to gene regulation through different intracellular signaling pathways (Taga & Kishimoto, 1997). In contrast to other members of the IL-6 family, IL-11 and IL-6 can activate cells through both classical and trans-signaling (Dayer & Choy, 2010; Lokau et al., 2016). During classical signaling, the ligand binds to the membrane-bound IL-11 or IL-6 receptor, while trans-signaling occurs when the ligand binds to its soluble form receptor before association with gp130 (Coles et al., 2007; Dayer & Choy, 2010). Soluble IL6 (sIL6R) and soluble IL11 (sIL11R) receptors naturally occur due to proteolysis of the membrane-bound receptor (Lokau et al., 2016; Müllberg et al., 1994). Additionally, sIL6R can be produced by alternative splicing as well (Horiuchi et al., 1994). Trans-signaling enables IL-11 to act on cells that express only gp130 but lack the IL-11 receptor, thereby further expanding the repertoire of cell types it can stimulate (Jones et al., 2001; Scheller et al., 2011). IL-11 classical signaling plays a decisive role in both physiological and pathological processes. It has a regulatory role in bone metabolism, in female fertility in mice, and has been associated with fibroinflammatory diseases (Agthe et al., 2017; Han et al., 2024; Ng, Dong, et al., 2020). In the case of trans-signaling, its biological role has not yet been identified. However, it has been shown that it is not required for normal skull development and female fertility in mice but may play a role in fibrosis (Agthe et al., 2017, 2018; Schafer et al., 2017).

1.4 Members of the IL-11 Signaling Complex

IL-11 exerts its effect by activating downstream signaling pathways through a signaling complex that comprises the IL-11Rα and the shared IL-6 family β receptor, gp130 (Metcalfe et al., 2023).

1.4.1 Interleukin-11

IL-11 is produced through the cleavage of a precursor consisting of 199 amino acids, which includes a leader peptide of 21 residues, resulting in a ~19 kDa protein that contains four α-helices (Airapetov et al., 2023; Akdis et al., 2011) (Figure 1). It has a high content of proline, leucine, and positively charged amino acids (Santos et al., 2008). The

helices are arranged in an up-up-down-down configuration comprising two pairs of antiparallel α-helices, which are connected by different lengths of peptide segments (Czupryn et al., 1995; Putoczki et al., 2014). Most of the connecting loops do not have a secondary structure, except for the AB loop, which includes a short alpha-helical part (Czupryn et al., 1995). The long loop between helices A and B makes specific interactions with helices B and D due to its localization across the surface of these helices (Putoczki et al., 2014). IL-11 lacks cysteine residues, which in other cytokines stabilize the helical structure (Czupryn et al., 1995; Neben & Turner, 1996; Rozwarski et al., 1994). However, the presence of hydrophobic amino acids at the interface formed by helices can compensate for the absence of disulfide bonds and stabilize the structure (Czupryn et al., 1995).

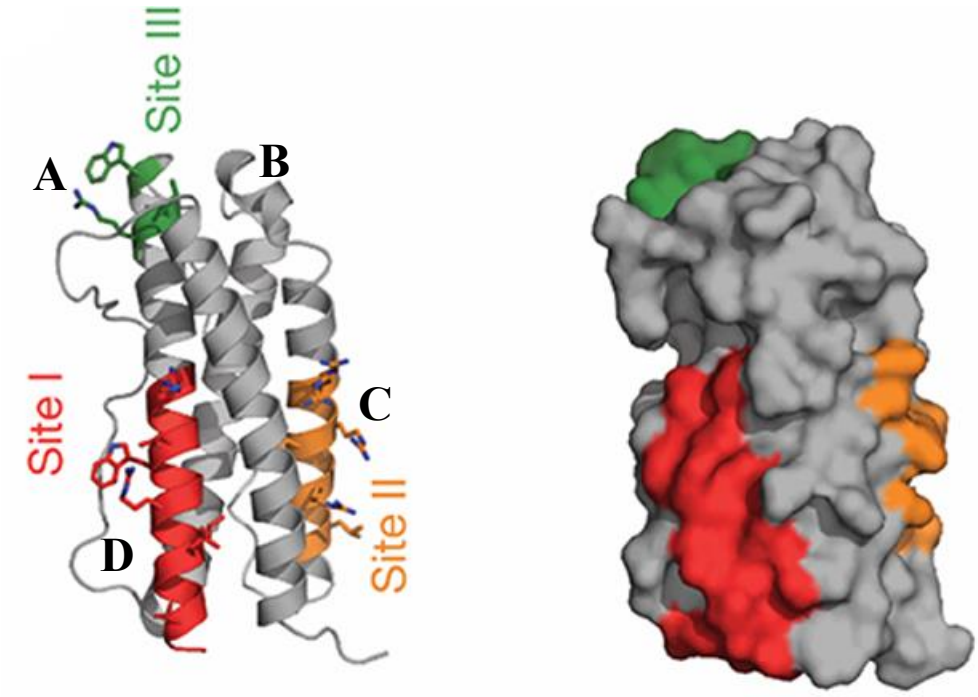

Figure 1. The structural presentation of the interleukin-11 cytokine. Adapted from (Metcalfe, Putoczki et al., 2020) The figures show the binding epitopes of IL-11: Site I (red), Site II (orange), and Site III (green). Site I binds the IL-11Rα, Sites II and III are involved in the binding of gp130.

1.4.2 Interleukin-11 Receptor

The IL-11 receptor is L-shaped, and the arrangement of its domains is similar to other IL-6 family cytokine receptors. The extracellular region of IL-11Rα (IL-11Rα_{EC}) comprises an N-terminal-Ig-like domain (D1) and two fibronectin type III domains (D2, D3) (Figure 2). Two disulfide bonds are present in D1 and D2 between cysteine amino

acids, and D3 has a conserved tryptophan-arginine ladder containing a strongly conserved WSXWS motif (Kohrs et al., 2025; Metcalfe, Aizel, et al., 2020). This motif is found in the ligand-binding chains and signal-transducing molecules of type I cytokine receptors and is essential for the generation of an adequately folded receptor (Hilton et al., 1996; Szabó et al., 2015). D1 is suggested to be a flexible domain. D2 and D3 regions form the cytokine-binding homology region (CHR), where IL-11 binds to the loops at the D2/D3 junction. The transmembrane domain is located at the C-terminal region of the molecule (Metcalfe, Aizel, et al., 2020).

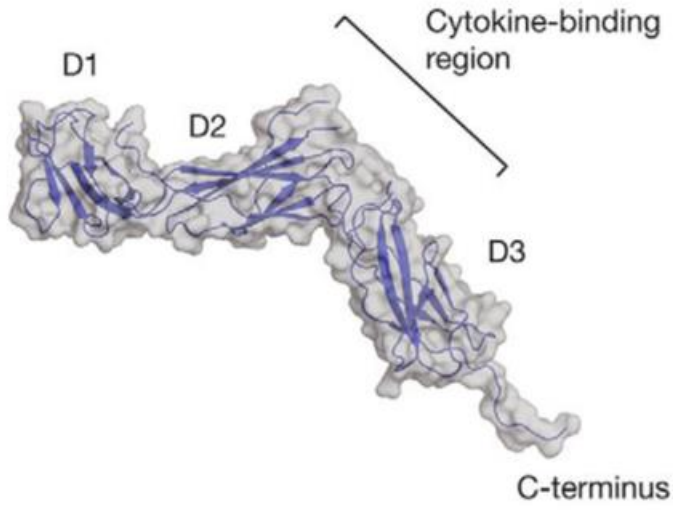

Figure 2. The structure of IL-11 receptor alfa (IL-11Rα). Reproduced from Metcalfe, Aizel, et al., 2020. The structure shows the D1, D2, and D3 extracellular domains of the IL-11Rα. The D2-D3 domains form the cytokine-binding domain. The transmembrane is located at the C-terminal region.

1.4.3 Glycoprotein 130

The 130kDa glycoprotein serves as the signal transducing receptor in the signaling complex (Metcalfe et al., 2023). The extracellular portion of the gp130 receptor has six domains. D1 is the N-terminal Ig-like domain, D2-D3 is the cytokine binding site (Figure 3), and D4-D6 is the membrane-proximal fibronectin type III domain (Kurth et al., 2000; Xu et al., 2010). The structures of these domains, except D1, minimally change after ligand binding (Xu et al., 2010). The linker between D1 and D2 allows for a slight conformational change, enabling the formation of the oligomeric complex. Furthermore, the D4-D6 domains are a dynamic signaling region that remains unstable after complex

formation and does not participate in its formation. However, these domains (D4, D5, D6) are considered responsible for the correct positioning of the transmembrane and intracellular domains of the two copies of gp130 (Metcalfe et al., 2023). Additionally, it influences the activation of the receptor and the intracellularly bound Janus tyrosine kinases (JAKs), which have a central role in the downstream signaling pathway (Hirano et al., 1997; Metcalfe et al., 2023; Morris et al., 2018). In addition to the proline-rich hinge region and cysteine residues, its cytokine binding region (CHR) also contains the highly conserved WSXWS motif (Bravo, 1998; Kohrs et al., 2025. Not only is the WSXWS the common feature of gp130 and IL-11Rα, but N-linked glycans are also visible on the signal transducer (Metcalfe et al., 2023).

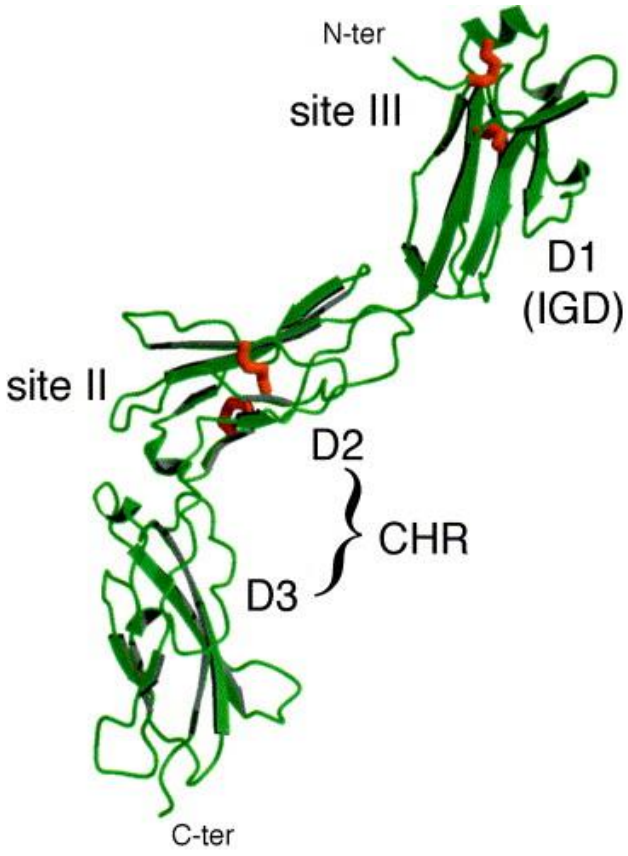

Figure 3. The structure of glycoprotein 130. Reproduced from Chow et al., 2002. The figure highlights its domains (D1, D2, D3), and specific binding sites (Site IIa, IIb, IIIa, IIIb) in different colors. The cytokine binding region (CHR) is composed of D2-D3. D4, D5, and D6 domains are not shown on the figure.

1.4.4 Interleukin-11 Signaling Complex

The IL-11 signaling complex is a hexamer containing two copies of IL-11, IL-11Rα, and gp130 (Metcalfe et al., 2023). As Metcalfe et al. described, the structure of the IL-11/IL-11Rα/gp130 complex can be imagined as a table, with IL-11, D2 domains of IL-11Rα, and gp130 being the top of the table and D3 domains of gp130 and IL11Rα at the legs. The rigid D5-D6 domains of two gp130 cross over as shown in the figure(Figure 4) and the D1-D2-D3 domains of each gp130 bind both the IL-11 receptor-cytokine complexes (Metcalfe et al., 2023).

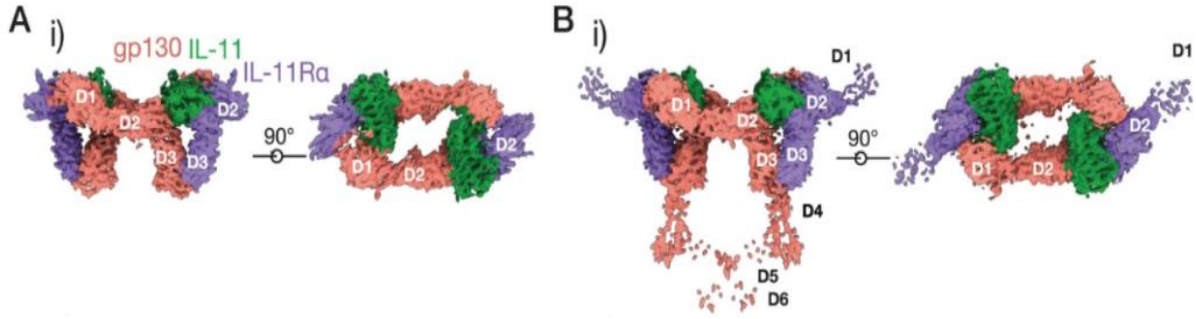

Figure 4. The structural representation of the interleukin-11 signaling complex, which includes IL-11 cytokine (green), IL-11 receptor α (purple), and the signal transducing subunit, gp130 (rose) (Modified from Metcalfe et al., 2023. D1 of IL-11Rα and gp130 receptors are the

Site-I of the cytokine mediates the formation of the IL-11-IL11Rα complex (1:1) and is formed by a hinge between the D2 and D3 domains of IL-11Rα (Gardner et al., 2024; Metcalfe et al., 2023). Gp130 interacts with the IL-11 – IL-11Rα complex through site-IIa and site-IIb. IL-11 interacts with one copy of gp130 at site-IIa, where the orientation of gp130 is stabilized by electrostatic interactions between residues of IL-11Rα with gp130, forming site-IIb (Gardner et al., 2024). The site-IIa interface is hydrophobic, located on helices A and C of IL-11, and mediated by four arginine residues of IL-11 and two loops of gp130. At site-IIb, the interaction is mediated by ten potential hydrogen bonds between D3 of IL-11Rα and D3 of gp130 (Metcalfe et al., 2023). D1 of gp130 mediates site-III interactions. Site-IIIa is where the second copy of gp130 binds to IL-11. Site-IIIa is stabilized by site-IIIb, where D1 of gp130 interacts with D2 IL-11Rα (Gardner et al., 2024; Metcalfe et al., 2023) (Figure 5). This site coordinates side chains across the complex (Gardner et al., 2024).

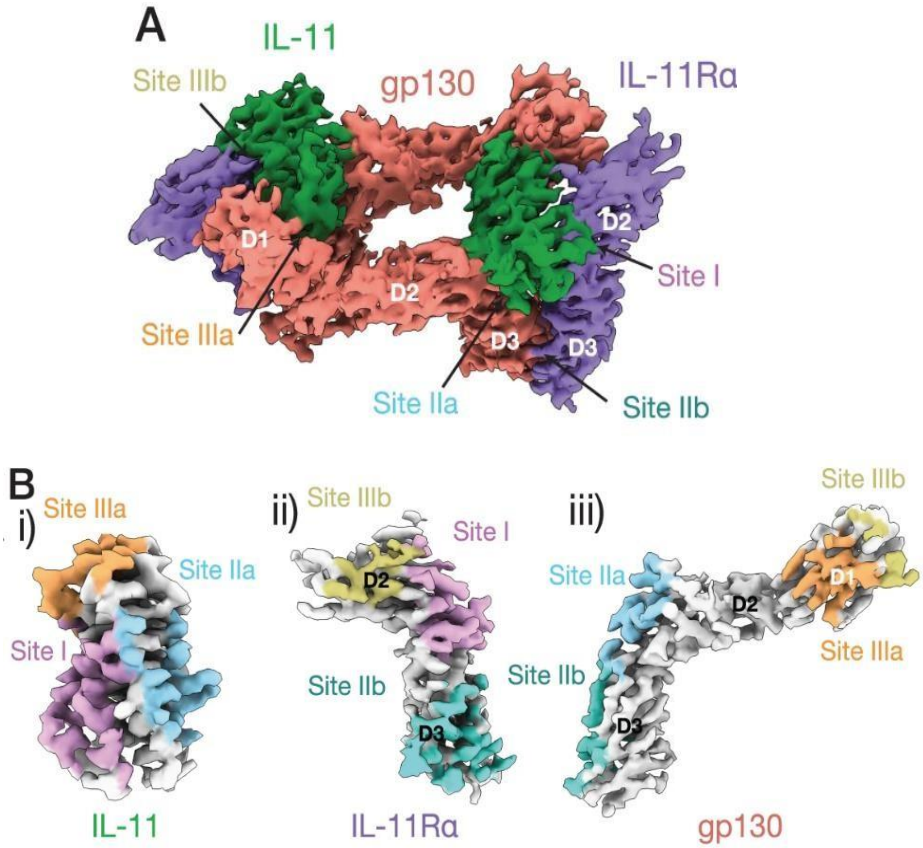

Figure 5. Interactions of IL-11 cytokine with IL-11Rα and gp130 receptors in the IL-11 signaling complex. Modified from Metcalfe et al., 2023. Figure A displays the full hexameric IL-11 signaling complex, highlighting the interactions between IL-11 (green), IL-11Rα (purple), and gp130 (rose). Figure B illustrates the specific interaction sites on each member of the signaling complex. Site-I mediates the interaction between IL-11 cytokine and IL-11Rα. Site-IIa and Site-IIb serve as interfaces between IL-11, IL-11Rα, and gp130. Site-III interactions involve the D1 domain of gp130 interacting with IL-11 and IL-11Rα, stabilizing the hexameric assembly essential for downstream signaling.

1.5 Role of Interleukin-11 in Health and Disease

Interleukin-11 is expressed in multiple tissues and has a pleiotropic function depending on which cell type it binds to (Du & Williams, 1997; O'Reilly, 2023). It is expressed in fibroblasts, mesenchymal stem cells, epithelial cells, hematopoietic cells, endometrial cells, osteoblasts, osteoclasts, central nervous system neurons, adipocytes, and cells in the gastrointestinal tract (Cork et al., 2001; Han et al., 2024; W. A. Silva et al., 2003). It participates in several physiological mechanisms; however, in healthy individuals, IL-11 expression is low or undetectable (Fung et al., 2022; Santos et al., 2008; Schafer et al., 2017). The isolation of IL-11 from marrow stromal fibroblasts suggested

its involvement in regulating bone marrow hematopoiesis (Paul et al., 1990). However, IL-11 signaling was dispensable for hematopoiesis in adult IL-11R-deficient mice, therefore, IL-11 may be unnecessary for hematopoiesis (Lokau et al., 2022; Nandurkar et al., 1997). Furthermore, loss of IL-11 signaling results in abnormal tooth number, skull disorders, and craniosynostosis, indicating its essential role in bone and tooth development (Nieminen et al., 2011). Interestingly, genetic deletion of IL-11 in mice extended their lifespan (Widjaja et al., 2024).

1.5.1 Role of Interleukin-11 in Fibrosis

IL-11 is associated with many diseases, including fibrotic diseases, different types of cancer, and inflammatory diseases (G. Huang et al., 2012; Ng et al., 2019; Nguyen et al., 2019; Nishina et al., 2021; Putoczki et al., 2013; Schafer et al., 2017).

The expression of fibroblast-specific IL-11 transgene or the injection of IL-11 in mice can lead to fibrosis in the heart, kidneys, and liver (Schafer et al., 2017; Widjaja et al., 2021). IL-11 was found to be expressed by lung stromal, epithelial cells, fibroblasts, and airway smooth muscle cells in response to viruses, cytokines, TGF-ß and histamine and contributed to the fibrotic responses by causing the local accumulation of fibroblasts, myofibroblasts, and collagen (Kortekaas et al., 2021; Tang et al., 1996). Moreover, in patients with idiopathic pulmonary fibrosis (IPF), IL-11 was upregulated and originated from fibroblasts (Ng et al., 2019). In addition, high levels of IL-11 were secreted by invasive IPF fibroblasts, whose phenotype is crucial for the progression of fibrosis (Geng et al., 2019).

The fibrotic effects of IL-11 are closely linked to the activation of the extracellular signal-regulated kinase (ERK) signaling pathway, similar to those induced by profibrotic cytokine transforming growth factor-beta (TGF-ß) (Schafer et al., 2017). It functions downstream of TGF-ß and exerts its profibrotic influence mainly at the protein level (Ng et al., 2019; Schafer et al., 2017). In vitro studies have demonstrated that IL-11 stimulates cellular processes in fibroblasts, including activation, migration, invasion, and enhanced collagen secretion by myofibroblasts, in an ERK-dependent manner (Ng et al., 2019). The presence of the autocrine signaling of IL-11 was confirmed by using the fusion protein of IL11Rα:IL11 (hyper IL11), which stimulates de novo synthesis and secretion of IL-11 via trans-signaling (Schafer et al., 2017). Different fibrotic factors, including TGF-ß, one

of the central players in fibrotic diseases, can stimulate this signaling pathway and increase IL-11 production in fibroblasts (Elias et al., 1994; Ng, Dong, et al., 2020; Ng et al., 2019; Schafer et al., 2017).

Interestingly, IL-11 or IL-11Rα knockout mice exhibited protection against fibrosis, suggesting that inhibition of the IL-11 signaling pathway could be a new target to treat fibrosis (Ng, Dong, et al., 2020; Ng et al., 2019, 2021; Schafer et al., 2017). Indeed, neutralizing antibodies blocking IL-11 in mice reduced fibrosis and reversed myofibroblast activation, meanwhile inhibiting ERK activation (Ng et al., 2019; Widjaja et al., 2021). Given its critical role in fibrotic diseases, inhibiting IL-11 signaling represents a promising therapeutic approach for treating them, including idiopathic pulmonary fibrosis.

1.6 Idiopathic Pulmonary Fibrosis

The lung is composed of epithelial, vascular, and stromal cells supported by specific tissue-resident immune cells, all vital for lung function and tissue repair (Ng et al., 2018; Schiller et al., 2019). While healthy lungs regenerate well after injury, chronic injury disrupts homeostasis, leading to persistent damage and scarring, known as fibrosis (Ng et al., 2018).

Idiopathic pulmonary fibrosis (IPF) is a chronic, irreversible disease that ranks as one of the most aggressive idiopathic interstitial pneumonias (IIPs) (Barratt et al., 2018; King et al., 2011). IPF is characterized by an abnormal extracellular matrix that drives lung remodeling, leading to the formation of scar tissue within the lungs (King et al., 2011; Meltzer & Noble, 2008). The disease affects millions of middle-aged and elderly adults worldwide, with a higher incidence in men (King et al., 2011; Richeldi et al., 2017). It initially represents symptoms of exertional breathlessness and dry cough (Meltzer & Noble, 2008). Its cause is unknown; however, multiple risk factors, including genetic and environmental factors (such as smoking and exposure to metal dust), recurrent micro-injuries, and aging, may contribute to the development of IPF (Meltzer & Noble, 2008; Richeldi et al., 2017). It is a serious condition characterized by a median survival of 2-3 years from diagnosis and limited treatment options (Collard et al., 2003; Moss et al., 2022; Raghu et al., 2011). Nintedanib and pirfenidone are the two approved orally administered antifibrotic drugs for treating IPF in the United States, Europe, and other countries (Glass

et al., 2022; Maher & Strek, 2019). Nintedanib acts by inhibiting receptor tyrosine-kinases, including fibroblast growth receptor (FGFR), vascular endothelial growth factors (VEGFR), and platelet-derived growth factor receptor (PDGFR), which mediate signaling pathways essential for the development of fibrosis (C et al., 2020). Currently, pirfenidone is known to have anti-inflammatory and anti-fibrotic effects by blocking the overexpression of type-I collagen and reducing the release of pro-inflammatory cytokines. However, its precise working mechanisms are not completely understood. (Torre et al., 2024). Both drugs can improve life quality, mitigate symptoms, and decelerate the disease's progression (Glass et al., 2022; Mei et al., 2022). However, they do not cure IPF, leaving lung transplantation as the only chance for survival (Glass et al., 2022; Mei et al., 2022; Singh et al., 2024). Moreover, only a few people can undergo this intervention due to the limited supply of organ donors and the risk of chronic allograft rejection (George et al., 2019; Mei et al., 2022).

1.6.3 Mechanisms Underlying the Pathogenesis of IPF

After injury, restoring tissue architecture is crucial for normal organ function (Wilson & Wynn, 2009). Therefore, the inability of dysfunctional tissue to regenerate is a significant factor in the progression of IPF (Barratt et al., 2018). The disrupted architecture of the lung leads to insufficient gas exchange, decreased lung capacity, and, finally, respiratory failure and death (Richeldi et al., 2017) (Figure 6).

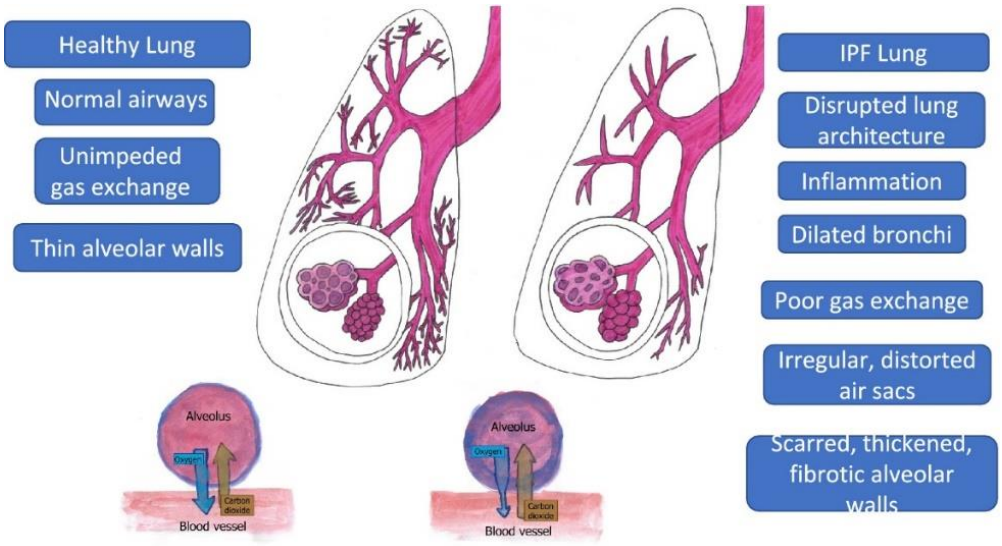

Figure 6. Comparison of a healthy lung and an IPF lung. Reproduced from Glass et al., 2022. The illustration shows the structural and functional differences between a healthy lung and a lung affected by idiopathic pulmonary fibrosis (IPF). Key differences include disrupted lung architecture, inflammation, dilated bronchi, irregular air sacs, and scarring of alveolar walls in the IPF lung, leading to poor gas exchange.

IPF is associated with the pathological pattern known as usual interstitial pneumonia (UIP), giving the lungs of IPF patients a heterogenous appearance with alternating areas of cystic fibrotic airspaces lined by bronchiolar epithelium (honeycomb cysts) and regions of healthy or minimally affected parenchyma (King et al., 2011; Meltzer & Noble, 2008). Although the understanding of its pathogenesis is incomplete, it is assumed that repetitive alveolar epithelial micro-injuries, including the injury of type II alveolar cells, and the subsequent activation of fibroblasts and myofibroblasts differentiation, play a central role (Camelo et al., 2014; Mei et al., 2022; Richeldi et al., 2017). Fibroblasts are diverse mesenchymal cells that maintain connective tissues during development and wound healing, thereby supporting essential organ functions (Grinnell, 2003; Plikus et al., 2021). Myofibroblasts are defined by their expression of smooth muscle alpha-actin and are the primary collagen producers in the lung (Tai et al., 2021; Tsukui et al., 2020). They are activated fibroblasts or derived from other cell types, such as epithelial and endothelial cells, or other mesenchymal precursors. Typically, they regulate tissue remodeling and wound healing. However, their persistent and pathological activation, as well as resistance to programmed cell death, contribute to the development of tissue fibrosis (Kis et al., 2011; Watsky et al., 2010).

Factors such as aging, genetics, environmental exposure, injury, and infections can damage the lung epithelium, leading to dysregulated activation of epithelial cells. The activated epithelial cells and macrophages secrete fibrogenic growth factors and cytokines, including TGF-ß (Fernandez & Eickelberg, 2012; Mei et al., 2022; Richeldi et al., 2017). In response to the secreted molecules, resident fibroblasts and bone marrow-derived progenitors (fibrocytes) migrate to the areas of micro-injuries, where they secrete and activate the latent TGF-ß (King et al., 2011). The activated TGF-ß stimulates the phenotypic switching of epithelial cells to mesenchymal cells (epithelial-mesenchymal transition (EMT) and endothelial-mesenchymal cell transition. Furthermore, it activates the differentiation of fibroblasts into myofibroblasts and the recruitment of macrophages (Fernandez & Eickelberg, 2012; King et al., 2011; Mei et al., 2022). Myofibroblasts produce an altered, stiff extracellular matrix (ECM) and exhibit abnormal collagen accumulation, contributing to myofibroblast activation in a positive feedback loop (Richeldi et al., 2017). The ECM produced in large amounts forms fibrotic lesions, known as fibroblastic foci (FF), which are the leading cause of fibrotic destruction and scarring in the lung (King et al., 2011; Mei et al., 2022; Richeldi et al., 2017).

1.7 Emerging Potential of Miniproteins in Targeted Therapies

Targeted approaches aiming at known molecular targets or pathways critical in a particular disease. This targeted pathway preferably does not overlap with other pathways, therefore reducing the risk of unwanted side effects (Popov & Schuppan, 2009). This approach includes function-blocking antibodies and small-molecule inhibitors (Gerber, 2008; Popov & Schuppan, 2009). Targeted therapies are essential due to their high specificity and ability to reduce adverse side effects (Asada et al., 2024).

1.7.3 Miniproteins

The primary amino-acid sequence determines the three-dimensional structure of a protein, influencing its interaction with other molecules. Thus, knowing proteins' structure from their amino acid sequence could help to determine their function and enable the design of new proteins with desired functions for novel biological tools and therapeutics (Paiva, 2024). David Baker, a world leader in protein design, has developed

computer-based methods and successfully designed new proteins. In 2024, he won the Nobel Prize for his significant contribution to computational protein design, which has revolutionized the biological and chemistry fields (Nobel Prize, 2024; Zhou et al., 2024).

Miniproteins are a diverse group of peptides characterized by small molecular size (1-10 kDa), two or more secondary structure elements, hydrophobic cores, and cooperative folding, wherein segments of the protein's structure influence each other to fold or unfold in an all-or-none manner, with minimal accumulation of intermediate states (Berger et al., 2024; Crook et al., 2020; Freire & Murphy, 1991; Malhotra & Udgaonkar, 2016). On one hand, they allow studying sequence-to-structure and structure-to-stability relationships in proteins. On the other hand, they represent useful miniprotein scaffolds incorporating functional domains, which are involved in protein-protein interactions and biomolecular binding (Baker et al., 2017). Protein engineering allowed the modification of naturally occurring proteins (P.-S. Huang et al., 2016). However, now it is feasible to design entirely new proteins, including miniproteins, from scratch to resolve challenges and pave the way for application in biotechnology and medicine (Baker et al., 2017; P.-S. Huang et al., 2016; Martin & Vita, 2000).

1.7.4 Therapeutic Potential of Miniproteins

Therapies utilizing miniproteins can achieve antibody-like affinity and functionality while addressing some limitations of large biologics. These include challenges such as tissue or cell penetration, complex manufacturing, sensitivity to proteases and reduction, and immunogenic potential. Miniproteins that occur naturally but lack the required serum half-life, cell penetration, and protease resistance properties can be chemically or genetically modified to meet the required features (Crook et al., 2020). Moreover, de novo protein design by computational methods enables the creation of stable miniproteins characterized by shapes customized to bind specific therapeutic targets (Berger et al., 2024; Cao et al., 2020; Chevalier et al., 2017). They have several advantages over monoclonal antibodies, including their capability to bind with high affinity even in a low picomolar range, and due to their small, stable structures, they can penetrate into tissues and act where larger proteins cannot (Asada et al., 2024; Crook et al., 2020). They can also withstand degradation in the gastrointestinal tract due to their stability and resistance to heat, acidic conditions, and proteolysis. Therefore, theoretically, even oral administration could be possible, allowing them to be absorbed

through the gut and reach the systemic circulation (Asada et al., 2024). Additionally, their size and stability could also allow nasal application or direct delivery into the respiratory system (Cao et al., 2020). Consequently, the accessibility to the treatment and the life quality of patients would improve. However, miniproteins have a relatively short half-life, likely due to their extraction through the kidney and liver. Despite this limitation, they can still achieve sufficient efficacy and safer treatment because of their high binding affinity, slow dissociation rate, and fewer side effects (Asada et al., 2024).

Computational protein design is a revolutionary technology that can provide alternative therapeutic strategies for treating various diseases. For instance, miniproteins have been designed to treat SARS-CoV-2 and cancer (Cao et al., 2020; Ham et al., 2024). A recent study has shown that orally administered designed miniproteins could serve as effective, safe, and low-cost therapies for autoimmune diseases by targeting cytokine signaling pathways through the inhibition of a specific ligand-receptor interaction (Berger et al., 2024). Furthermore, in a lung fibrosis mouse model, a de novo designed integrin inhibitor protein reduced the severity of fibrosis, indicating the therapeutic potential of de novo designed proteins (Roy et al., 2023). According to Cao et al., the main challenge of this approach is not necessarily the de novo design of proteins with the appropriate chemical and shape properties, but recognizing the best miniprotein candidates (Cao et al., 2020). The design of miniproteins using computational tools has an emerging role in drug discovery. Nonetheless, it is important to emphasize that drug discovery continues to rely on “wet lab” techniques and laboratory screening methods. Therefore, advanced in vitro experiments remain essential for successful drug discovery (Baker et al., 2017; Berger et al., 2024; Crook et al., 2020). Thus, developing miniproteins combining computational tools with state-of-the-art laboratory techniques to target molecules that are key players in the fibrotic mechanisms could lead to the development of potential new drugs to treat fibrotic diseases such as IPF (Roy et al., 2023).

2 Chapter 2

Article

Development of IL-11 receptor-targeting miniproteins to cure Idiopathic Pulmonary Fibrosis

Komporday K.1,2, Masa Cs2., Kremlitzka M2., Murányi J2.,Gordos A2., Oroszlan.G2*,

1 University of Algarve, 8005-139 Faro, Portugal

2 VRG Therapeutics Zrt.- 1083, Budapest, Hungary

*Corresponding author: gabor.oroszlan@vrgtherapeutics.com

Abstract: Idiopathic pulmonary fibrosis (IPF) is a chronic, progressive interstitial lung disease characterized by excessive extracellular matrix accumulation, lung tissue stiffening, and irreversible loss of function, leading to high mortality rates. Current treatments are only moderately effective, highlighting the urgent need for new therapeutic strategies. Interleukin 11 (IL-11, a cytokine in the IL-6 family) plays a significant role in fibrosis by activating fibroblasts and promoting collagen secretion via its receptor complex, consisting of IL-11 receptor alpha (IL-11Rα) and the signal transducer glycoprotein 130 (gp130) receptor. Targeting IL-11 signaling thus represents a promising strategy to slow fibrotic progression and enhance outcomes. This study aims to design new, computationally generated miniproteins that specifically target IL-11Rα to inhibit IL-11 signaling. Miniproteins are advantageous over traditional small molecules and biologics due to their compact size, high stability, and antibody-like affinity and selectivity, which enhance tissue penetration and manufacturing efficiency. A library of 400 novel miniprotein scaffolds was designed and displayed on M13 bacteriophages for biopanning and in vitro assays. Due to challenges in obtaining sufficient receptor yield in-house using mammalian expression system (HEK293-F cells), a commercially available IL-11Rα was used for screening and validation. Four rounds of phage display resulted in significant enrichment of IL-11Rα miniprotein binders. Two candidates, DN226 and DN213 demonstrated strong, specific binding in ELISA assays and competed effectively with IL-11 cytokine for its receptor binding site. DN226 exhibited superior affinity and competitiveness against IL-11 cytokine compared to DN213. These findings validate the miniproteins' potential to disrupt IL-11 signaling. This work highlights the integration of AI-driven de novo protein design with state-of-the-art phage display and in vitro assays as an effective platform for discovering potential IL-11Rα inhibitors. DN226 represents a promising hit molecule for novel anti-fibrotic therapeutics in IPF. Future studies are proposed to optimize miniprotein properties and evaluate in vivo efficacy.

Keywords: de novo protein design, idiopathic pulmonary fibrosis, IL-11 signaling, miniproteins, phage display

2.2 Introduction

Idiopathic pulmonary fibrosis (IPF) is a chronic, progressive interstitial lung disease characterized by extensive extracellular matrix deposition, disruption of alveolar architecture, and irreversible loss of lung function. The hallmark of IPF is excessive lung fibrosis leading to stiffening of lung tissue, impaired gas exchange, and ultimately, respiratory failure with high mortality rates (Barratt et al., 2018; Richeldi et al., 2017). Despite recent therapeutic advances, effective treatments remain limited, and the complete molecular mechanism driving IPF is not fully understood, underscoring the need for novel interventions (Mei et al., 2022; Singh et al., 2024).

Cytokine-mediated communication plays a fundamental role in maintaining physiological homeostasis, immune response, and tissue regeneration (Curfs et al., 1997; Dinarello, 2007; Liu et al., 2021). Cytokines are small, short-lived proteins secreted by various cell types, including macrophages, lymphocytes, stromal cells, and natural killer cells (Liu et al., 2021; Rose-John, 2018). The biological effects of cytokines are highly context-dependent, as a single cytokine can elicit diverse responses in different target cells depending on receptor expression patterns and intracellular signaling environments (Hirano et al., 1997; Tenney et al., 2005). This complexity is demonstrated by the IL-6 family cytokines and the gp130 receptor system. Cytokines can be categorized into various subgroups based on their specificity, structure, and the receptor complexes with which they interact. For instance, members of the interleukin-6 family share one or, in the case of IL-11 and IL-6, two copies of the signaling receptor subunit, gp130 (Rose-John, 2018)

IL-6 family includes several members. Among them, IL-11 has gained attention due to its role in fibrotic diseases (Ng et al., 2019; Schafer et al., 2017; J. Zhou et al., 2025). IL-11, a 19 kDa protein, was initially identified in immortalized fibrocyte-like bone marrow stromal cells (Airapetov et al., 2023; Nguyen et al., 2019) IL-11 signals through a heterodimeric complex made up of IL-11Rα and gp130. It binds specifically to IL-11Rα while gp130 functions as the signal transducer subunit (Akdis et al., 2011; Rose-John, 2018). Upon binding to its receptor, this receptor complex forms and enables the activation of downstream signaling pathways, including the JAK/STAT and MAPK pathways (Han et al., 2024; Metcalfe et al., 2023). IL-11 can activate cells either via

classical signaling by binding the membrane-bound IL-11Rα or through trans-signaling by interacting with its soluble IL-11 receptor (Han et al., 2024).

The effects of IL-11 are pleiotropic and vary depending on the target cell type (O'Reilly, 2023). Initial studies linked IL-11 to hematopoiesis; however, further research using mouse models suggested that IL-11 signaling is dispensable for hematopoiesis (Lokau et al., 2022; Nandurkar et al., 1997; Paul et al., 1990). Instead, IL-11 plays an essential role in skeletal and dental development (Nieminen et al., 2011). Furthermore, it may contribute to aging processes as the genetic deletion of IL-11 in mice increased their lifespan (Widjaja et al., 2024). In healthy tissues, its expression is typically low or undetectable (Nguyen et al., 2019; Schafer et al., 2017). However, IL-11 was shown to be upregulated in multiple pathological conditions, including IPF, where its levels correlate with disease severity (Ng et al., 2019).

Expression of IL-11 results in fibrosis in multiple organs, including the lungs, heart, and kidneys (Ng, Cook, et al., 2020; Schafer et al., 2017). The primary source of IL-11 appears to be the fibroblasts in response to other cytokines (Ng et al., 2019; Nguyen et al., 2019; Schafer et al., 2017). In IPF, IL-11 plays a critical role in promoting fibroblast activation, migration, invasion, and collagen secretion (Ng et al., 2019). Moreover, IL-11 contributes to chronic inflammation and cellular senescence in the lung by activating the JAK/STAT and nonclassical MAPK pathways (Zhou et al., 2025). Animal models deficient in IL-11 or IL-11Rα show protection from fibrosis, and antibody-mediated blockage of IL-11 significantly reduces fibrosis and myofibroblast activation (Ng et al., 2019, 2021; Schafer et al., 2017). Therefore, targeting IL-11 signaling represents a promising therapeutic strategy for fibrotic diseases, such as IPF (Ng et al., 2021; Schafer et al., 2017).

The human lung comprises a complex interplay of epithelial, vascular, stromal, and immune cells, which coordinate lung functions and repair mechanisms (Ng et al., 2018; Schiller et al., 2019). While lung tissue has a remarkable regenerative capacity, repeated and chronic injury disrupts tissue homeostasis, leading to pathological remodeling and inflammation (Ng et al., 2018). IPF is a chronic progressive lung disease characterized by repetitive epithelial injury, chronic activation and invasion of fibroblasts, and excessive accumulation of collagen (Mei et al., 2022; Moss et al., 2022). Environmental factors, aging, and genetics can increase the risk of developing IPF; however, the exact mechanism underlying the disease's pathology remains unclear (Mei

et al., 2022; Ng et al., 2018). Treatment options are limited, and despite the best medical care, the median survival time is only 2-3 years after diagnosis (Barratt et al., 2018; Moss et al., 2022). Anti-inflammatory agents have failed to enhance clinical outcomes, and the two FDA-approved anti-fibrotic drugs, nintedanib and pirfenidone, are associated with toxicity and do not cure the disease (Mei et al., 2022; Ng et al., 2019).

The rising recognition of IL-11's central role in fibrogenesis suggests that targeted blockade of IL-11 signaling could represent an innovative therapeutic approach for IPF. Targeted therapies focus on specific critical molecular pathways implicated in disease, aiming to minimize side effects by avoiding interference with unrelated pathways (Asada et al., 2024; Popov & Schuppan, 2009). Among emerging therapeutic methods, miniproteins —peptides with well-defined tertiary structuresm disulfide bonds and/or hydrophobic core ranging from 1 to 10 kDa— have gained interest due to their versatile structure-function relationships and potential as scaffolds for modulating protein-protein interactions (Baker et al., 2017; Berger et al., 2024; Crook et al., 2020). Advances in computational protein design, recognized by David Baker's Nobel Prize in 2024, have enabled the de novo creation of miniproteins with customized shapes and high-affinity binding capabilities (Cao et al., 2022; Nobel Prize, 2024; Y. Zhou et al., 2024). Computational approaches enable the targeting of specific binding sites on protein surfaces, resulting in a more precise and efficient method for designing binders and library screening methods (Cao et al., 2022). Miniproteins combine antibody-like specificity with enhanced tissue penetration and stability under harsh conditions, suggesting possibilities for non-invasive administration routes, such as nasal delivery. Although challenges like short serum half-life exist, miniproteins exhibit slow dissociation rates and reduced immunogenicity and side effects, facilitating safer and effective treatments (Asada et al., 2024; Crook et al., 2020). Recent studies highlight their potential application in antiviral, anticancer, autoimmune, and antifibrotic therapies (Berger et al., 2024; Cao et al., 2020; Roy et al., 2023). Besides the role of computational protein design in accelerating drug discovery, it is essential to emphasize the importance of state-of-the-art laboratory work and in vitro experimental validation, which are still crucial components for successful drug discovery and development (Baker et al., 2017; Berger et al., 2024; Crook et al., 2020).

Phage display can be used to identify and select miniprotein scaffolds with high affinity and specificity for their target. Its core elements are phages, which can infect bacteria and display a library of amino acid sequences. It is based on the genetic modification of the phage DNA by integrating DNA sequences of interest into a specific DNA sequence in the phage genome, which encodes one of the phage coat proteins, thereby enabling the display of peptides, proteins, or antibodies on its surface. During screening methods, scaffolds with the highest binding affinity for their target molecule can be selected for further testing and validation steps. This technique is a powerful tool for studying protein interactions and discovering new protein sequences (Jaroszewicz et al., 2022).

This work aims to identify functional miniprotein scaffolds that target the IL-11 receptor, competing with the IL-11 cytokine, to develop potential drug candidates with high specificity and binding affinity. After using bioinformatic tools to design the miniprotein scaffolds, phage display technique is applied to screen and select the most potential candidate. In parallel, IL-11Rα constructs are designed for the mammalian expression system and serve as target receptors in in vitro assays to validate the binding efficacy and functionality of the miniproteins.

2.3 Material and Methods

2.3.3 DNA Manipulation

2.3.3.1 DNA Library Preparation

The IL-11Rα constructs were designed using bioinformatics tools, like SnapGene and commercially available AA sequences, and ordered from AcroBiosystems. Miniproteins targeting IL-11Rα were designed using AI-driven structural bioinformatics tools, including RFdiffusion, ProteinMPNN, and AlphaFold2.The in silico-designed miniprotein scaffold library was ordered as an "oligo pool", which contained 400 different single-stranded oligonucleotide sequences, thereby allowing their simultaneous screening. All target DNA fragments were amplified in a 50 µL reaction using PCR (ProFlex^{TM} 96-well PCR System, Applied Biosystems, Cat. No.: 4484075)) using primers designed with SnapGene software. PCR products were verified and separated by agarose gel electrophoresis. The band with the expected size was cut out, and DNA fragments were extracted using Macherey-Nagel NucleoSpin Gel and PCR Clean-up kit. DNA fragments and vector backbones were digested by Thermo Fisher Scientific's FastDigest restriction enzymes and 10x FastDigest Green buffer to generate compatible ends for cloning.

2.3.3.2 Cloning

Digested IL-11Rα DNA fragments were ligated into pcDNA3.1 for expression in FreeStyle 293 F cells. Digested miniprotein DNA fragments were ligated into pAS62 phagemid vector for phage display application. T4 DNA ligase from Thermo Fisher's Rapid DNA Ligation kit was used to catalyze the formation of phosphodiester bonds between the digested and purified plasmid backbone and insert. The molar ratio between the vector DNA and insert was 1:3 for pcDNA3.1 and 1:10 for pAS62 vector. A negative control was used for each ligation that did not contain any insert to check for the presence of undigested or self-circularized plasmid backbone in the sample. The following equation was applied to calculate the appropriate amount of insert for 100 ng of vector DNA:

Amount of insert [ng] = 3 amount of plasmid DNA [ng]*Size of insert [bp]/ Size of backbone DNA [bp]*

Ligated constructs were used immediately for bacterial transformation or stored until further use.

2.3.3.3 Bacterial Transformation and Plasmid Preparation

During my experiments, two *Escherichia coli* (*E. coli)* strains were used, the NEB 10-beta and NEB 5-alpha from New England Biolabs. NEB 10-beta cells were premade chemically competent Mix & GO cells following the Mix & GO! *E. coli* transformation kit, thereby simplifying the transformation process. The cells were cultivated in LB medium complemented with antibiotics. A pre-mixed powder by Invitrogen was used to prepare the Luria-Bertani (LB) medium, LB agar, and 2x Yeast Extract Tryptone medium (2YT). NEB 10-beta premade Mix&Go *E. Coli* cells were transformed with pcDNA3.1 plasmid DNA containing the IL-11 receptor gene following Zymo Research's high-efficiency transformation Mix & GO competent cells protocol (C3019H). NEB 5-alpha E. coli cells were transformed with a miniprotein DNA library following a New England Biolabs' high-efficiency transformation protocol (C2987H). Plasmid DNA containing the IL-11Rα gene was extracted using the Macherey-Nagel NucleoSpin Plasmid purification kit or the Macherey-Nagel NucleoSpin Plasmid Midiprep purification kit.

2.3.4 Protein Expression

A sterile environment was maintained, and the risk of contamination was minimized during experiments. For this reason, all work with mammalian cells was carried out in a horizontal safety cabinet using sterilized equipment.

2.3.4.1 Basic handling of FreeStyle 293-F (HEK) cell line

For experiments, the FreeStyle human embryonic kidney (HEK293-F) cells were used to produce IL-11Rα. FreeStyle-293-F cell line derived from the HEK293 cell line purchased from Thermo Fisher Scientific. HEK293-F cells were maintained and grown in 30 mL serum-free FreeStyle 293 expression medium (Thermo Fisher Scientific, Cat. No.:12338018) according to the manufacturer's protocol in a 37°C incubator with a humidified atmosphere of 8% CO2 in air on an orbital shaker rotating at 125 rpm. For general maintenance, the cells were passed when they reached 1-3 x 10^6 viable cells/mL.

2.3.4.2 Passaging Cells

FreeStyle 293-F cells were passed every 3-4 days to avoid nutritional depletion and maintain cell viability. Cells were centrifuged for 5 minutes at 500 g. Supernatant was discarded, and the cell pellet was resuspended in 30 mL FreeStyle 293 expression medium (Thermo Fisher Scientific, Cat. No.: 12338018). For general cell maintenance, an anti-clumping agent (Thermo Fisher Scientific, Cat. No.: 0010057AE) was added to the cells to reduce cell clumping and achieve higher viable cell densities in the cell suspension. Before transfection, no anti-clumping agent was added to the cells, because it can interfere with the transfection process.

2.3.4.3 Transfection of FreeStyle 293-F cells

The cells were maintained in FreeStyle 293 expression medium (Thermo Fisher Scientific, Cat. No.: 12338018) throughout the procedure. Before transfection, cell density and cell viability were determined by trypan blue exclusion, ensuring over 90% viability and a single cell suspension. For each transfection, 3 x 10^7 viable cells were suspended to reach the 1 x 10^6 cells/mL concentration in 30 mL of medium. Transient protein expression was carried out to produce IL-11 receptor protein in HEK293-F cells. Plasmid DNA transfection was performed on cultured cells using 293fectin transfection reagent (Thermo Fisher Scientific, Cat. No.: 12347019). Suspension HEK293-F cells were transfected according to Thermo Fisher Scientific's Transfection protocol. The cells were maintained in FreeStyle 293 expression medium (Thermo Fisher Scientific, Cat. No.: 12338018) throughout the procedure.

2.3.4.4 Harvesting cells and supernatant post-transfection

Two, three, and five days after transfection, the produced protein was harvested from the supernatant. First, the cells were centrifuged for 5 minutes at 500 g. On the first day of harvesting, the cell pellet was resuspended in 30 mL of FreeStyle 293 expression medium (Thermo Fisher Scientific, Cat. No.:12338018) for further protein production. On the last day of transfection, the cells were not resuspended. The culture supernatant was collected, and a second centrifugation was performed at 4000 g for 15 minutes to remove any residual cellular particles. The clarified supernatant was then collected into low-protein-binding tubes for downstream protein purification and analysis.

2.3.4.5 Protein Purification

After harvesting the cell and supernatant, the supernatant containing the IL-11Rα was purified for Sodium Dodecyl Sulfate Polyacrylamide Gel (SDS-PAGE) electrophoresis. Supernatant centrifuged 15000 G, Filtered with 0,22 μm PES syringe filter, purified using Ni- IMAC 5ml, and size-exclusion column.

2.3.4.6 SDS-PAGE and Western Blot

First, samples were diluted in Tris-Glycine SDS sample buffer (2x) (Thermo Fisher Scientific, Cat. No.:LC1676). SDS-PAGE was performed using 4–20% Tris–Glycine gels (Novex™ Tris-Glycine Mini Protein Gels, 4–20%, 1.0 mm, WedgeWell™ Invitrogen, Cat. No.: XP04200BOX) and 1× Tris–Glycine SDS running buffer (Thermo Fisher Scientific, Cat. No.: LC2675-4) following the manufacturer's guidelines. The proteins were then transferred to nitrocellulose membranes (Nitrocellulose/Filter Paper Sandwich, 0.2 μm, 8.3 x 7.3 cm, Thermo Fisher Scientific, Cat. No.: LC2000) and probed with an anti–6×His monoclonal antibody diluted 1:2500 (Invitrogen, Cat. No.: MA1-135) and a horseradish peroxidase (HRP)-conjugated goat anti-mouse secondary antibody (Abcam, Cat No.: ab97040), diluted 1:2500 as specified by the manufacturer.

2.3.4.7 In-house IL-11 Cytokine Production

The recombinant IL-11 cytokine used in downstream assays was previously produced in-house using the same method described above for IL-11Rα.

2.3.5 Phage Display System

P3 phage monovalent display system was used to screen the miniprotein library and select the promising candidates for further in vitro assays.

2.3.5.1 Phage propagation

Following recovery from the transformation of NEB 5-alpha *E. coli* cells, the remaining 800 μL of the transformation mixture was transferred into 2YT medium supplemented with ampicillin. Cultures were incubated at 37 °C with shaking at 250 rpm until an optical density at 600 nm of 2.0 was reached. M13KO7 helper phage (from New England Biolabs, Cat. No.:18311019) was added to the culture. After adding the helper phage, the cultures were incubated for 30 minutes at 37 °C at 250 rpm. Afterwards, the

cultures were transferred into 25 mL of 2YT medium containing carbenicillin and kanamycin and incubated overnight at 37 °C with shaking at 250 rpm. The following morning, phages were precipitated and purified for the screening assay.

2.3.5.2 Phage Precipitation and Purification

After phage propagation, bacterial cells were removed from culture by centrifugation at 8000 g for 15 minutes at 4 °C. The supernatant containing phage particles was carefully transferred into a fresh tube, and 2.5 M NaCl/20% PEG-8000 (w/v) was added to precipitate phages. After 3 minutes of incubation, phage particles were pelleted by centrifugation at 18,000 g for 15 minutes at 4 °C. Supernatant was discarded, and a low-speed centrifugation was performed at 1000 rpm for 1 minute at 4 °C to remove any residual liquid. The phage pellet was then carefully resuspended in 2 mL of Dulbecco's phosphate-buffered saline (DPBS) (Thermo Fisher Scientific, Cat. No. :14190250) containing bovine serum albumin (BSA, Sigma-Aldrich, Cat.No.: A2153) and Polysorbate (Tween 20, Sigma-Aldrich, Cat. No.:P9416) (BSA-DPBST) for further experiments.

2.3.5.3 Biopanning

2.3.5.3.1 Screening

A Nickel-coated black 96-well plate (Pierce™ Nickel Coated Plates, Black, 96-Well, Thermo Fisher Scientific Cat.No.: 15342) was used for the screening procedure of the de novo miniprotein library. The screening procedure followed a series of binding, washing, and elution steps. IL-11Rα can bind the Nickel-coated surface of the plate due to the HIS-tag. The nickel-coated plate was coated with 0,15 µg/well IL-11Rα diluted in DPBS (Thermo Fisher Scientific, Cat. No.: 14190250) and incubated for 1 hour at RT with gentle shaking. After, the BSA-DPBST (DPBS: Thermo Fisher Scientific, Cat. No.: 14190250), BSA: Sigma-Aldrich, Cat.No.: A2153, Tween 20: Sigma-Aldrich, Cat. No.:P9416) solution was added to cover any remaining uncoated sites on the plate. This prevents non-specific binding of phages directly to the plate, ensuring that they bind the immobilized IL-11Rα. To know the right volume of phage solution to be diluted in BSA-DPBST, the concentration was determined by using Nanodrop at 269 nm and 320 nm and by applying the following equation:

$$virions/mL = (A_{269}\text{-}A_{320}) * 6 \times 10^{16} / number\ of\ bases/virions$$

After 1 hour of incubation, the phage library solution, diluted in BSA-DPBST, was added to each well containing the target receptor and incubated for 1 hour. Then the wells were washed 4 times in the first and second round and 8 times in the third and fourth round with 0,05% PBST (PBS Buffer (10x), Serva Cat. No.: 4259501) using an automated plate washer. Bound phages were eluted by adding 100 nM Glycine buffer (pH 2,7) and incubated for 5 minutes at RT. Then, the eluate was collected from each row into separate Eppendorf tubes and neutralized by adding 1 M Tris buffer (pH 7,6)

2.3.5.3.2 Phage Titering

Phage titering was performed by first growing NEB 5-alpha cells in 2YT medium supplemented with tetracycline at 37 °C until an OD between 2 and 4 was reached. 900 µL of cultured cells was added into seven wells per sample in a deep well plate and incubated at 37 °C with shaking at 250 rpm until further use. Serial dilutions of eluted phage samples were prepared in a 96-well plate by transferring the samples across seven wells containing 2YT medium, thereby achieving dilution factors ranging from 10-10^7. After, each diluted phage sample was added to the corresponding wells containing the NEB 5-alpha cells in the deep well plate and incubated for 5 minutes at 37 °C with shaking at 250 rpm to allow the infection. Finally, the infected cultures were plated onto agarose plates containing carbenicillin and incubated overnight at 37 °C. The following morning, the plates were evaluated, and plaques were enumerated. The enrichment factor was calculated by comparing the phage titer in the experimental wells, containing the target molecule (IL-11R), relative to the control well.

2.3.5.4 Propagation Phage Clones

Propagating phage clones was a necessary step to produce a sufficient number of purified clones for individual validation in ELISA assays. After determining the number of individual clones to expand, for each colony to be expanded, 500 µL of 2YT medium containing ampicillin and 5 µL of helper phage dilution were prepared in individual tubes. Colonies were picked with sterile pipette tips, first streaked onto an ampicillin-agar plate to maintain traceability, and then inoculated into the tubes. The inoculated colonies were incubated overnight at 37 °C with shaking to ensure efficient mixing, bacterial growth, and phage propagation.

2.3.6 Peptide Preparation

Promising peptides were subcloned from pAS62 vector into pET45b vector with BamHI and XhoI restriction enzymes, containing an N-terminal histidine affinity tag and a WELQ protease cleavage site. Peptides were expressed in BL21 (DE3) *E. coli* cells overnight at 22 °C, induced using Isopropyl β-D-thiogalactopyranoside (IPTG), sonicated, and lysed afterward. The cell supernatant was purified by combining Immobilized Metal Affinity Chromatography, dialysis, SPLB cleavage, Ion Exchange chromatography, and Size Exclusion Chromatography, yielding 95%+ pure miniproteins.

2.3.7 Enzyme-linked immunosorbent assays

2.3.7.1 Indirect sandwich ELISA for IL-11 receptor validation

Indirect sandwich ELISA was designed to detect the interaction between immobilized IL11Rα, produced in FreeStyle 293-F cells, and in-house produced IL-11 cytokine, thereby functionally validating IL11Rα. First, 0,15 µg of IL11Rα diluted in PBS was coated onto a Nickel-coated 96-well microplate (Pierce™ Nickel Coated Plates, Clear, 96-well, Thermo Fisher, Cat. No.: 15442) through the receptor's HIS-tag and incubated for 1 hour at RT with gentle shaking for receptor immobilization onto the surface. For negative control groups, wells were not coated with IL11Rα, or Hyper IL-6 (0,15 µg/well) was coated onto the plate. Nonspecific binding sites were blocked with 250 µL of BSA-DPBS (1% BSA in DBPS containing 0,05% Tween-20, DPBS: Thermo Fisher Scientific, Cat. No.: No.:14190250, BSA: Sigma-Aldrich, Cat.No.: A2153, Tween 20: Sigma-Aldrich, Cat. No.:P9416) for 1 hour at RT with gentle shaking to reduce background noise. Different concentrations of IL-11 cytokine, diluted in BSA-DPBST, were added to the wells and incubated for 1 hour at RT with gentle shaking to bind the immobilized IL11Rα. Following three washes with PBS-Tween to remove unbound cytokines, the wells were incubated for 1 hour at RT with gentle shaking with 50 µL of primary anti-IL-11 antibody (anti-hIL11 antibody from R&D Systems, Inc Bio-Techne, Cat. No.: AB-218-NA) diluted 1:2000 in 1% BSA-PBST to detect the IL-11 cytokine-IL11Rα complex. After three additional washes, HRP-conjugated anti-goat secondary antibody (anti-goat IgG-HRP antibody from R&D Systems , Inc Bio-Techne, Cat. No.: HAF017) was applied to detect the bound primary antibodies. After the final washing steps, 100 µL of TMB substrate (1-Step Ultra TMB-ELISA, Thermo Scientific, Cat. No.:

34028) was added and incubated for 7 minutes before stopping the reaction with 50 µL of 1 M HCl. The absorbance was recorded at 450 nm using a SpectraMax iD3 microplate reader. The Kd value, a measure of receptor-ligand binding affinity of IL-11Rα was calculated in GraphPad Prism 8 using a one-site total and nonspecific binding nonlinear regression.

2.3.7.2 Phage ELISA

A direct sandwich ELISA was employed to evaluate the binding of phage-displayed miniproteins to immobilized IL-11Rα on nickel-coated 96-well plates (Pierce Nickel Coated Plates, Clear, 96-well, Thermo Fisher, Cat. No.: 15442). The first two steps were the same as for the ELISA described above. Phage supernatant, containing phage-displayed miniproteins, was diluted in 1% BSA-PBST and added to the wells and incubated for 1 hour at RT with gentle shaking. After washing four times with PBS-Tween to remove unbound phages, anti-M13 IgG antibody (Invitrogen, Cat. No.: MA5-36125) was diluted 1:2500 in blocking buffer and added. Colorimetric detection was performed in the same way as described above.

2.3.7.3 Competitive ELISA

Competitive ELISA was performed to analyze the competitiveness between the phage-displayed miniproteins, or peptides, and IL-11 cytokine for IL11Rα using Nickel-coated 96-well plates (Pierce^{TM} Nickel Coated Plates, Clear, 96-well, Thermo Fisher, Cat. No.: 15442) . The protocol used a workflow similar to the indirect sandwich ELISA to assess IL-11 functionality. However, when the IL-11 cytokine was incubated in a mixture with phage supernatants, only anti-M13 IgG antibody (Invitrogen, Cat. No.: MA5-36125) was used to detect phages bound to the receptor through miniproteins displayed on their surfaces. When the peptide was added to a mixture with cytokine, anti-hIL11 antibody diluted in 1:2000, and anti-goat IgG-HRP antibodies diluted in 1:2000 (R&D Systems, Inc., Bio-Techne, Cat. No.: HAF017 Systems) were used in the same way as described above. Detection steps were the same. The optimal concentration of IL-11 cytokine for competitive ELISA assays was determined based on its Kd (~6 nM), measured in-house in accordance with literature data (Curtis et al., 1997; Metcalfe et al., 2023), using a one-site total and nonspecific binding nonlinear regression in GraphPad Prism. The Ki values were calculated using one-site fit Ki nonlinear regression in GraphPad Prism 8.

2.4 Results

Our primary goal was to design miniprotein drug candidates that target the same binding site on IL-11Rα as the IL-11 cytokine, thereby inhibiting the IL-11 signaling pathway. IL-11Rα was designed and produced in mammalian cells for in vitro assays, in which it serves as an immobilized target molecule for the miniprotein scaffolds. The following section will demonstrate the results of the mammalian expression system and the validation of the produced receptor. Following that, it will describe the screening results of the phage display biopanning campaign and the validation of the binding effectiveness and specificity of selected miniprotein scaffolds.

2.4.3.1 Detecting the expressed IL-11Rα

The successful PCR amplification and cloning of the IL-11Rα gene into pcDNA3.1 were confirmed by Sanger sequencing. Then, this plasmid was used to transfect HEK293-F cells to produce the encoded receptor in the mammalian system. The expression of His-tagged recombinant IL-11Rα (rIL-11Rα) in HEK293-F cells was verified by SDS-PAGE electrophoresis and Western Blot analysis. We collected samples from the cell culture supernatant on days 3 and 5 post-transfection for SDS-PAGE and Western Blot analyses. Additionally, cell lysate supernatant was collected for Western Blot. To compare our results, in-house rIL-11Rα was used as a positive control for SDS-PAGE, and commercial IL-11Rα with a His-tag (cIL-11Rα, from AcroBiosystems) at 0.1 and 0.2 μg/μL for Western Blot. Purified receptor samples were also tested in SDS-PAGE electrophoresis.

2.4.3.2 SDS-PAGE Electrophoresis

As shown in Figure 7 SDS-PAGE gel image showed one protein band corresponding to the expected molecular weight of the glycosylated recombinant IL-11Rα (~50 kDa) in the purified IL-11Rα sample (fraction 5). Detectable bands were not observed in the remaining receptor samples or in the positive control sample. However, faint bands were detected near the loading wells, suggesting protein aggregation.

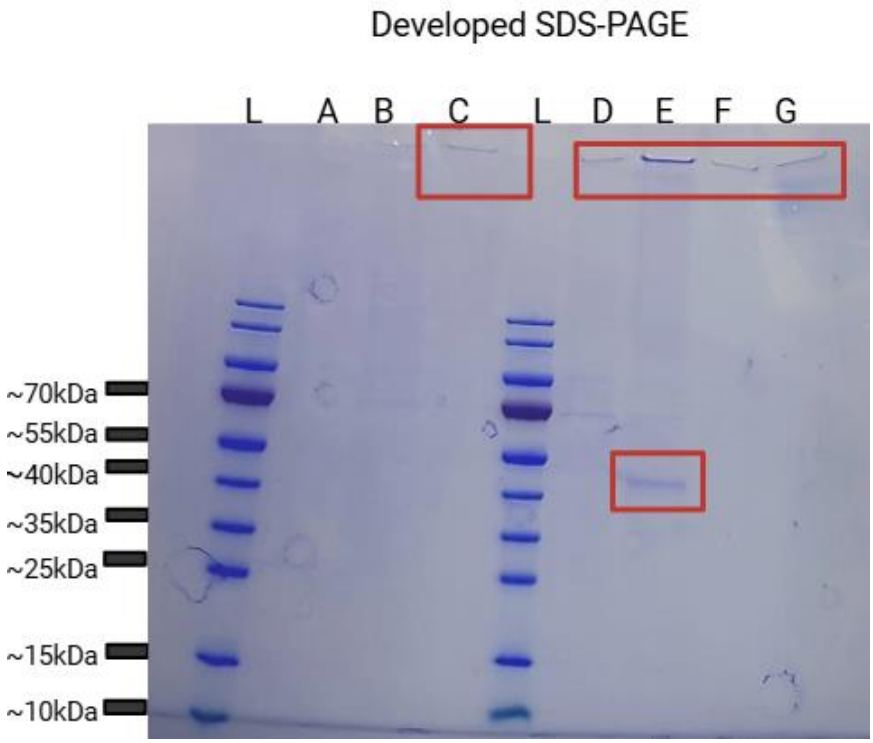

Figure 7. Image from developed SDS-PAGE. L: PageRuler Plus Prestained protein ladder A: sample of day 3 supernatant B: sample of day 5 supernatant C: purified IL-11Rα supernatant D: purified IL-11Rα flow-through E: purified IL-11Rα fraction 5 F: purified IL-11Rα fraction 6 G: positive control

2.4.3.3 Western Blot

After SDS-PAGE electrophoresis, a Western blot was performed using anti-His tag monoclonal antibody and an anti-goat secondary antibody conjugated to HRP. Figure 8 shows the developed Western blot. Distinct protein bands consistent with the expected molecular weight of rIL-11Rα (~50 kDa) were observed, with intensity increasing proportionally to protein concentration (0.1µg/µl to 0.2 µg/µl). This confirmed the antibody efficacy and successful blotting. In the 3-day supernatant samples, the lane is more visible compared to the 5-day sample; however, in both cases, only faint bands were visible at ~ 45-50 kDa, indicating low expression levels. In the cell lysate samples, faint bands can be detected, suggesting low intracellular rIL-11Rα levels as well

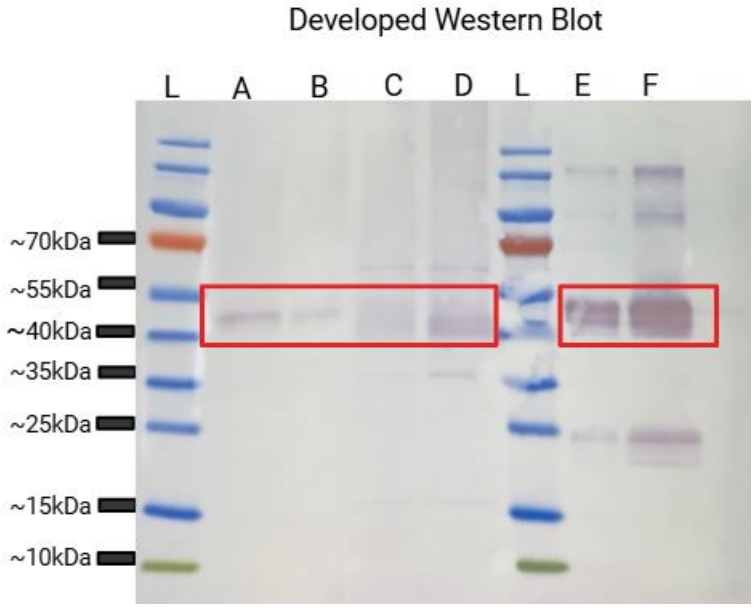

Figure 8. Image from a developed Western Blot, detecting the produced rIL-11R**α.** L: PageRuler Plus Prestained protein ladder A: sample of day 3 supernatant B: sample of day 5 supernatant C: sample of day 3 cell lysate D: sample of day 5 cell lysate E: 0.1 ug/ul IL-11Rα F: 0.2 ug/ul IL-11Rα.

Considering these results, HEK293-F cells expressed rIL-11Rα; however, only in small amounts, and a significant portion was probably aggregated.

2.4.4 Validating the Expressed IL-11Rα by in vitro assay

The rIL-11 receptors were functionally validated using a highly sensitive sandwich enzyme-linked immunosorbent assay (ELISA). This assay tested interaction with previously produced in-house tag-free IL-11 cytokine, detected with a polyclonal antibody against IL-11 (anti-hIL11 antibody) and a secondary antibody linked to HRP (anti-goat IgG HRP antibody). The rIL-11Rα receptor was coated onto the microplate surface (0.15 µg/well), and its ability to bind IL-11 cytokine was measured at 450 nm. The binding activity of the rIL-11Rα was compared to that of the His-tagged cIL-11Rα. As shown in Figure 9, at a concentration of 200 nM IL-11 cytokine, the cIL-11Rα showed a higher absorbance signal (A=0,69) compared to the rIL-11Rα (A=0.43), indicating stronger ligand binding. Similarly, at a 20 nM cytokine concentration, the cIL-11Rα demonstrated a higher signal (A = 0.61) than the rIL-11Rα (A = 0.25). At the lowest cytokine concentration, both receptors displayed similarly low absorbance values (cIL-11Rαr: A=0.2; rIL-11Rα:A= 0.19).

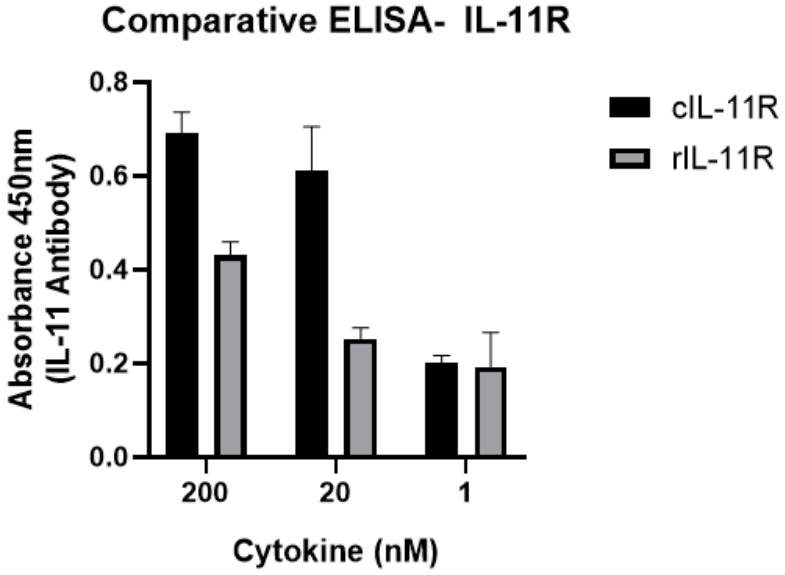

Figure 9. Comparative ELISA of commercially available IL-11R (cIL-11R) and in-house recombinant IL-11R (rIL-11R). The binding of IL-11 cytokine to IL-11 receptors was measured at 200 nM, 20 nM, and 1 nM cytokine concentrations. Absorbance at 450 nm, detecting anti-IL-11 antibody, shows higher binding for cIL-11R compared to rIL-11R at higher cytokine concentrations, while at the lowest concentration tested, a comparable binding was detected. The graph was generated in GraphPad Prism 8.

These data indicate that the rIL-11Rα was functionally active and capable of binding the IL-11 cytokine, although it achieved a lower signal compared to the cIL-11Rα. Therefore, for further in vitro studies, the commercial receptor was used due to the insufficient amount of rIL-11Rα and the higher functional activity of the cIL-11Rα.

The cIL-11Rα was individually tested using a binding ELISA assay for functional validation before being used in further in vitro experiments. Increasing levels of IL-11 cytokine were employed to evaluate the binding efficiency of cIL-11Rα. As demonstrated in Figure 10, cIL-11Rα showed a dose-dependent binding pattern consistent with rising cytokine concentrations, confirming the receptor's functionality. The negative control (BSA) exhibited no significant specific binding. The Kd of cIL-11Rα determined from our ELISA experiment was 6.436 nM.

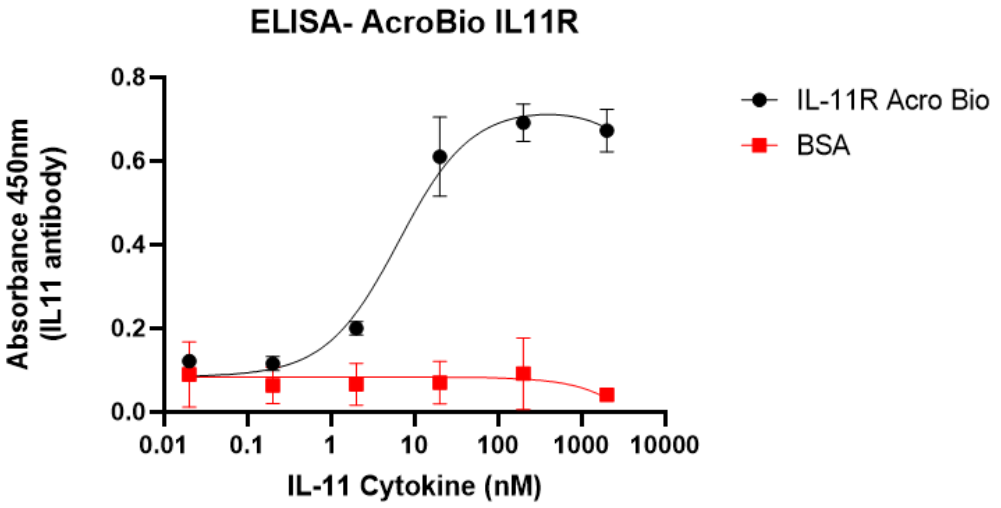

Figure 10. ELISA binding assay of IL-11 cytokine to cIL-11R (from AcroBio). Increasing concentrations of the IL-11 cytokine were tested for binding to cIL-11R (black line) compared with a BSA control (red line). Absorbance was measured at 450 nm after detection with anti-IL-11 antibody. IL-11R shows a dose-dependent binding curve, while the negative control shows no significant binding. The graph was generated in GraphPad Prism 8.

2.4.5 Phage Display System

The de novo designed miniprotein library was successfully cloned into the pAS62 vector and validated with New Generation Sequencing. The plasmid library was used to transfect NEB 5α cells and for phage propagation using M13KO7 helper phage. After successful phage precipitation and purification, the phages were used in screening rounds to select and enrich miniprotein scaffolds that can potentially bind IL-11Rα.

2.4.5.1 Enrichments of screening rounds

The enrichment of miniproteins across four rounds of screening was analyzed, evaluating the increase in eluted phages compared to the control group, BSA. As shown in Figure 11 progressive enrichment was detected by the increasing number of eluted phages from the receptor compared to BSA from round 1 to round 4. In the first two rounds, the enrichment was minimal, with values of 2.71 for round 1 and 1.15 for round 2. An increase was observed in round 3, with the enrichment factor reaching 22. The most visible enrichment occurred in the fourth round, yielding an enrichment ratio of 187. This increase indicated a successful enrichment of phages displaying potential miniproteins that can bind to the cIL-11Rα. These results confirmed that four rounds of biopanning could lead to a successful selection process, enriching the number of phages that specifically bind to the target, cIL-11Rα.

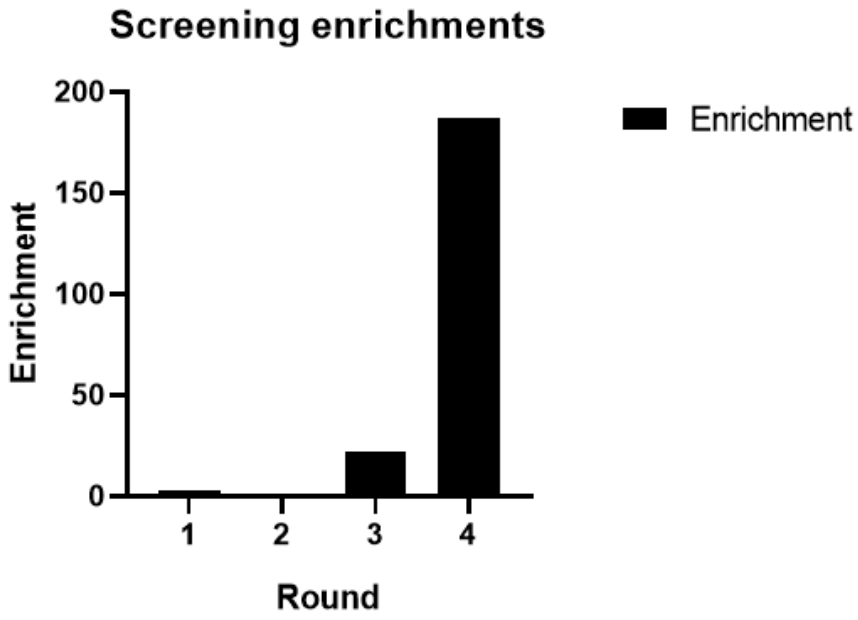

Figure 11. Screening enrichments. The figure shows the enrichment throughout the 4 rounds of biopanning. An increase was observed in round 3, reaching 22, and significantly rose to 187 in round 4. The graph was generated in GraphPad Prism 8.

2.4.6 Enzyme-linked Immunosorbent Assays

After four rounds of phage biopanning screening, two single phage clones (DN226, DN213) were successfully isolated from the biopanning process by picking 10-20 different colonies from the agarose plate. After NGS sequencing, these two scaffolds were identified as the most frequently occurring. The clones were amplified individually for detailed characterization. These hits were subjected to Sanger sequencing and then profiled using phage ELISA.

2.4.6.1 Phage Binding ELISA

A direct phage sandwich ELISA was conducted to confirm the binding between DN226 and DN213 miniproteins displayed on phage and cIL-11Rα. Serial dilutions of phages (from 1.50 x 10^{11} to 2.06 x 10^{8} pfu/well) were incubated on cIL-11Rα-coated microplates (0.15 μg receptor /well). Negative controls without cIL-11Rα assessed nonspecific binding. As shown in Figure 12, the binding pattern of DN226 displayed on phage showed a concentration-dependent increase, with the highest absorbance value of 3,095 observed at the highest phage concentration (1.50 x 10^{11} pfu/well). At the lowest

phage concentration level (2.06 x 10^8 pfu/well), the absorbance was 0.133. In contrast, negative control groups displayed minimal absorbance across all phage concentrations. This result indicates the selective interaction between DN226 miniprotein and its target, IL-11Rα.

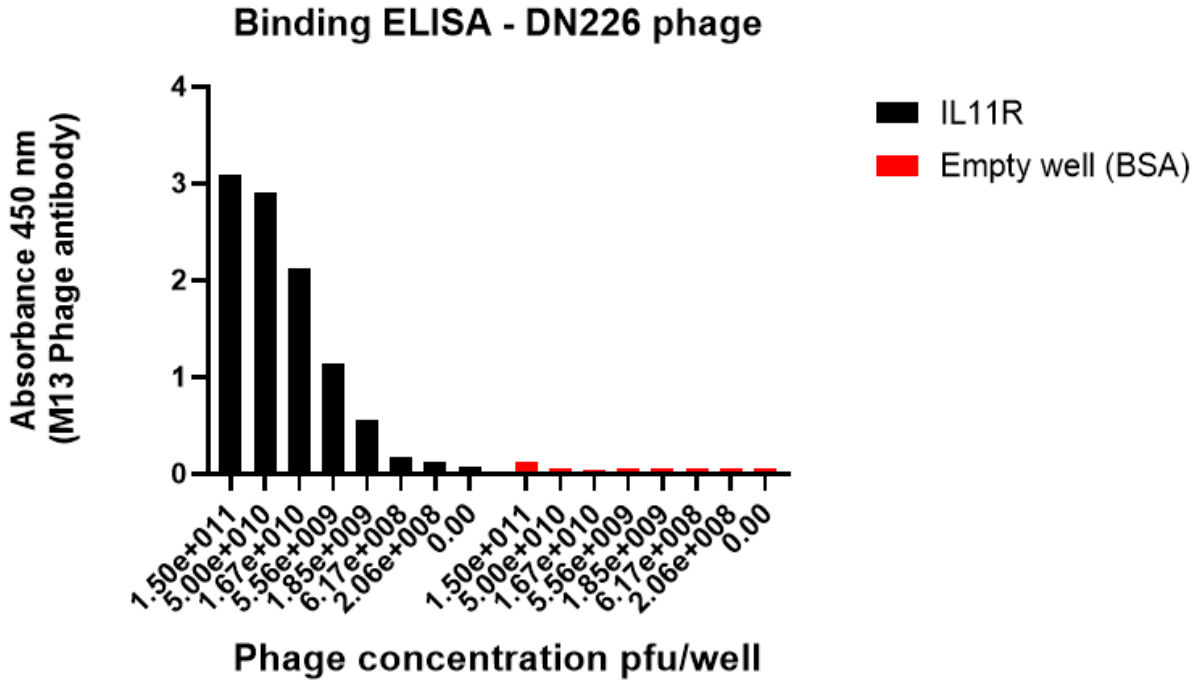

Figure 12. Phage binding ELISA of DN226 miniprotein. The "y" axis shows the absorbance values detected at 450 nm. The "x" axis shows the different phage concentrations (PFU/well. DN226 binding was measured at varying phage concentrations (pfu/well) using IL11R-coated wells (black bars) compared to empty wells blocked with BSA (red bars). Binding was detected with anti-M13 phage antibody and measured as absorbance at 450 nm. DN226 shows a concentration-dependent binding to IL-11R. The graph was generated in GraphPad Prism 8.

DN213 exhibited a strong, concentration-dependent binding to IL-11Rα as well, as demonstrated in Figure 13.At the highest concentrations (1.5×10^{11} to 5×10^{10} pfu/well), absorbance at 450 nm exceeded 3.0, indicating interaction with the receptor. Binding levels decreased with lower phage concentrations, reaching an absorbance of 0,515 at 2×10^8 pfu/well. Negative controls showed negligible absorbance at all tested concentrations, close to baseline, confirming minimal nonspecific interactions between DN213 and the well surface or assay reagents. Compared to DN226, DN213 exhibited slightly higher absorbance at the highest phage concentrations.

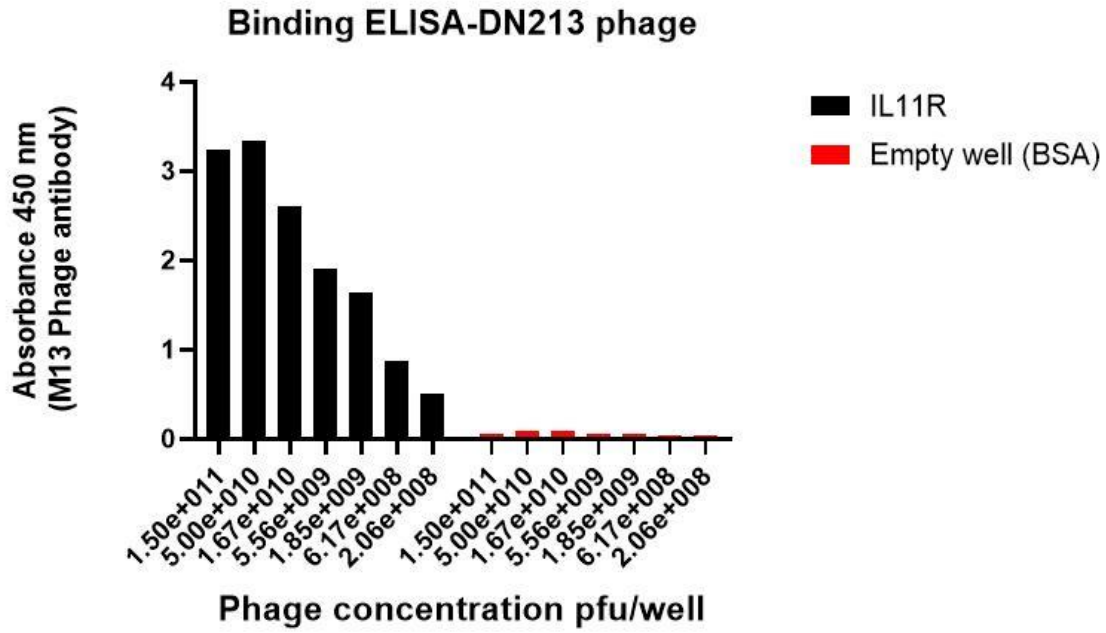

Figure 13. Phage binding ELISA of DN213. The "y" axis shows the absorbance values detected at 450 nm. The "x" axis shows the different phage concentrations (PFU/well). DN213 binding was measured at varying phage concentrations (pfu/well) using IL11R-coated wells (black bars) compared to empty wells blocked with BSA (red bars). Binding was detected with anti-M13 phage antibody and measured as absorbance at 450 nm. DN213 shows a concentration-dependent binding to IL-11R. The graph was generated in GraphPad Prism 8.

These results confirmed that both DN226 and DN213 miniproteins could bind the IL-11Rα target with strong affinity when displayed on the phage surface. For this reason, DN226 and DN213 were further tested using competitive ELISA to assess a more detailed analysis.

2.4.6.2 Competition Between Miniproteins and IL-11 Cytokine

A competitive direct ELISA was implemented to assess the efficiency of competition between miniproteins (DN226, DN213) and IL-11 cytokine for binding to IL-11Rα, thereby determining whether the miniproteins bind specifically to the binding patch of the cytokine on the receptor. The microplate was coated with cIL-11Rα (0.15 µg/well) or BSA for negative controls and incubated with a constant concentration of phages displaying DN226 or DN213 in the presence of increasing IL-11 cytokine concentrations. An anti-M13 phage antibody was used to detect the binding between phage-presented miniproteins and IL-11Rα. The optimal concentration of IL-11 cytokine for competitive ELISA assays was determined based on its Kd (~ 6 nM).

2.4.6.2.1 Phage Competitive ELISA

As shown in Figure 14, DN226 exhibited a strong signal in the absence of the IL-11 cytokine, with an absorbance value of 1.99, indicating the binding between DN226 and cIL-11Rα. The addition of 50 nM IL-11 cytokine reduced the binding between the miniprotein and the receptor, as demonstrated by a reduced absorbance level (A = 1.434). Furthermore, in the presence of 250 nM cytokine concentration, the phage binding was almost completely abolished. In contrast, the negative control group exhibited a minimal absorbance at all cytokine concentrations, indicating the lack of nonspecific binding.

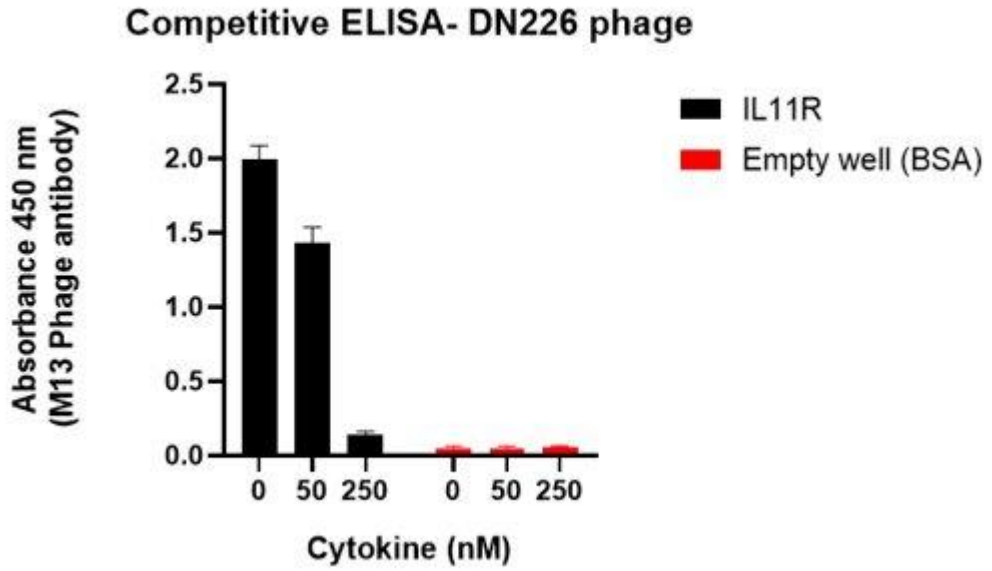

Figure 14. Competitive ELISA detecting the competition between DN226 miniprotein displayed on phage and IL-11 cytokine for the target IL-11Rα. The cytokine was added at concentrations of 50 and 250 nM. The "y" axis shows the absorbance values at 450 nm, detecting the M13 Phage antibody. Binding of DN226 phage to IL-11R (black bars) was assessed in the presence of increasing concentrations of IL-11 cytokine (0-50-250 nM). Phage binding was detected using M13 antibody at 450 nm. Increasing cytokine concentrations reduced DN226 binding to IL-11R in a dose-dependent manner, indicating competitive binding. The negative control group (red bars) exhibited a minimal absorbance at all cytokine concentrations. The graph was generated in GraphPad Prism 8.

In the case of DN213, IL-11 cytokine concentrations of 5 nM and 50 nM were applied. Compared to DN226, DN213 had a lower binding efficacy towards cIL-11Rα, with an absorbance of 1.00 in the absence of IL-11 cytokine (Figure 15). In the presence of 5 nM IL-11 cytokine, the absorbance values reduced to 0.74. At a 50 nM cytokine concentration, the binding between DN213 and cIL-11R was almost completely diminished. The negative controls showed a slightly higher signal compared to the DN226 negative groups; however, it still indicates a negligible nonspecific interaction.

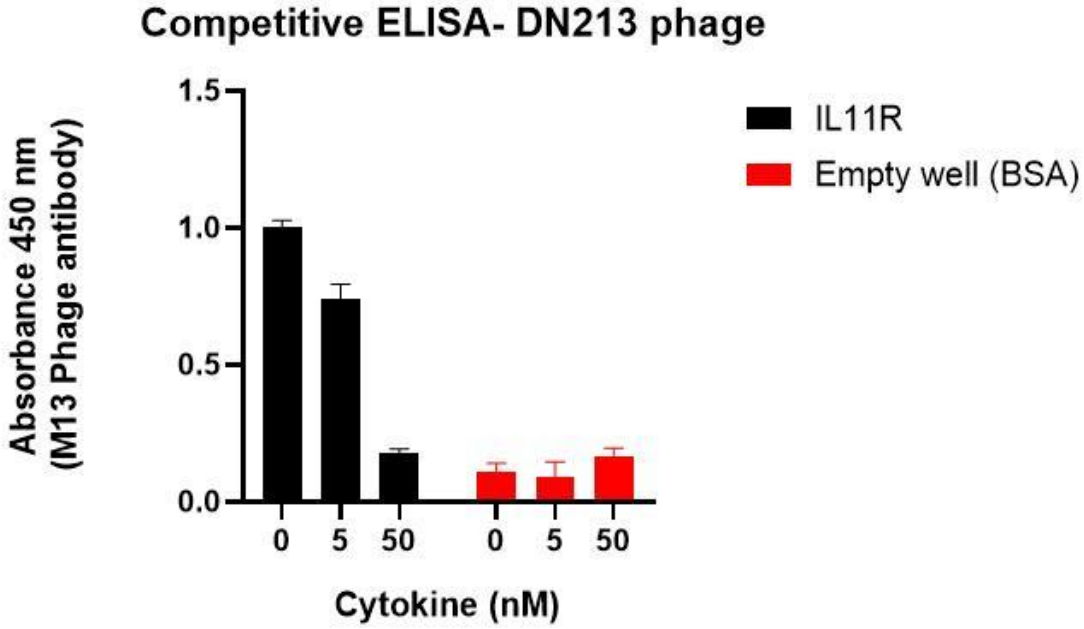

Figure 15. Competitive ELISA detecting the competition between DN213 miniprotein displayed on phage and IL-11 cytokine for the target IL-11Rα. Binding of DN213 phage to IL-11R (black bars) was assessed in the presence of increasing concentrations of IL-11 cytokine (5-50 nM). Phage binding was detected using M13 antibody at 450 nm. Cytokine concentrations reduced DN13 binding to IL-11R in a dose-dependent manner, indicating competitive binding. The negative controls (red bars) showed very low absorbance signal across all conditions. The graph was generated in GraphPad Prism 8.

2.4.6.2.2 Competition between DN226 or DN213 peptides and IL-11 cytokine

For further characterization, both DN226 and DN213 were produced as peptides and analyzed following the indirect competitive ELISA method. An anti-hIL-11 antibody and an anti-goat IgG-HRP antibody were applied to detect the binding of IL-11 cytokines to the receptor. The peptides were applied at different concentrations, while the IL-11 cytokine concentration was kept at 10 nM.

2.4.6.2.2.1 DN226 Peptide Explorative Competitive ELISA

As shown in Figure 16, 10,000 nM of DN226 peptide reduced the signal from absorbance values of 0.716 to 0.27, indicating that the DN226 peptide could compete with the IL-11 cytokine and bind cIL-11Rα effectively at the cytokine binding site.

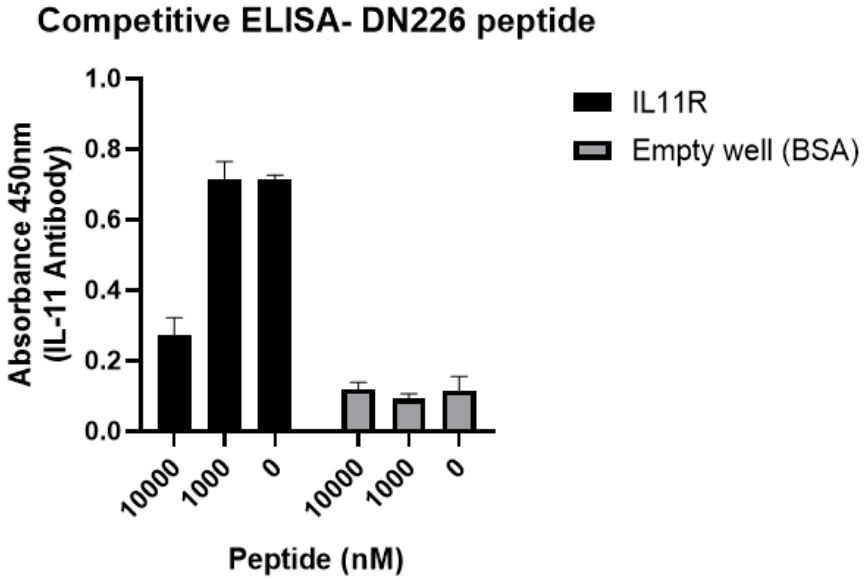

Figure 16. Competitive ELISA of DN226 peptide with IL-11 cytokine to bind IL-11Rα. The "x" axis shows the peptide concentration (nM), and the "y" axis displays the absorbance values at 450 nm, detecting the IL-11 antibody binding. The binding of IL-11 was assessed in the presence of the DN226 peptide at different concentrations (10,000 nM and 1,000 nM) and in the absence of the peptide. At the highest peptide concentration (10,000 nM), a significantly reduced signal was measured compared to the no-peptide control, indicating competitive binding (black bars). Negative control (grey bars) showed minimal absorbance across all concentration levels. The graph was generated in GraphPad Prism 8.

2.4.6.2.2.2 DN213 Peptide Explorative Competitive ELISA

In the case of DN213 peptide, the competition between the peptide and the cytokine was unsuccessful because 10,000 nM of DN213 peptide caused only a slight reduction of the signal, with absorbance values of 0,41 from absorbance of 0.54 detected in the absence of the peptide (Figure 17). This indicated that the DN213 peptide could bind the cIL-11Rα less effectively compared to DN226. Negative controls display a slight increase, suggesting some level of unspecific binding.

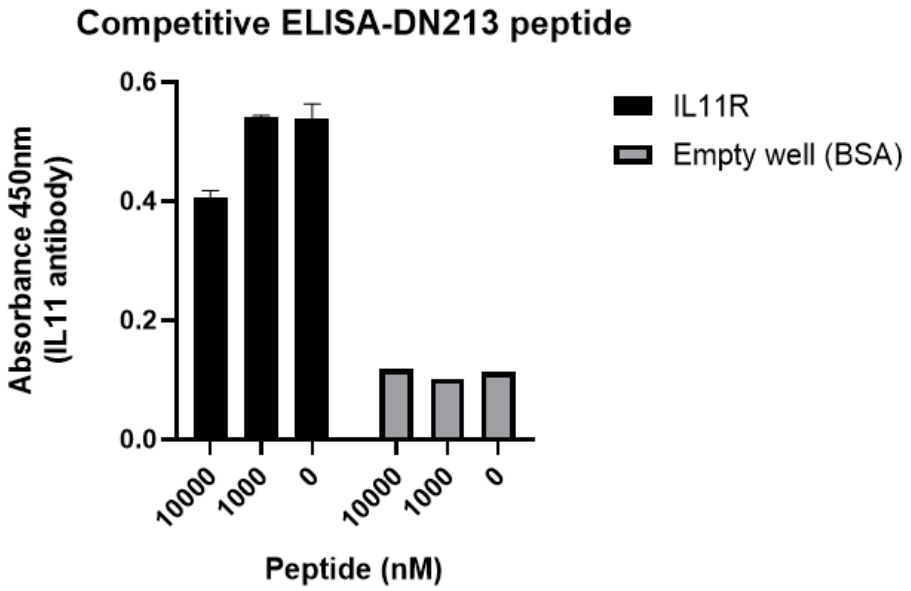

Figure 17. Competitive ELISA of DN213 peptide with IL-11 cytokine to bind IL-11Rα. The "x" axis shows the peptide concentration (nM), and the "y" axis displays the absorbance values at 450 nm, detecting the IL-11 antibody binding. The binding of IL-11 was assessed in the presence of DN213 peptide at different concentrations (10,000 nM, 1000 nM) and in the absence of the peptide. At the highest peptide concentration (10,000 nM), a moderately reduced signal was measured compared to the no-peptide control (black bars). Negative control (grey bars) showed minimal absorbance across all concentration levels. The graph was generated in GraphPad Prism 8.

These results suggest that the DN226 peptide is a stronger binder that can target IL-11Rα specifically and with high affinity. Therefore, a more in-depth evaluation was conducted using this peptide at multiple concentrations.

2.4.6.2.2.3 DN226 Peptide Competitive ELISA

To further characterize binding efficiency, a detailed ELISA measurement was carried out, yielding a saturation curve. IL-11 cytokine at 10 nM concentration was competed against increasing concentrations of DN226 peptide for receptor binding. IL-11 cytokine was detected to assess the interaction between IL-11 cytokine and cIL-11Rα. As shown in Figure 18. The binding curve demonstrates a concentration-dependent decrease in absorbance with increasing peptide concentration. The highest absorbance value (A = 0.406) was reached at a 10 nM peptide concentration, which then sharply decreased starting from a 1000 nM DN226 peptide concentration, reaching the lowest absorbance of 0.1 at a 30,000 nM peptide concentration. In contrast, the negative control group showed consistently low absorbance across all tested concentrations. This assay confirmed that DN226 can compete with IL-11 cytokine for binding to IL-11Rα, thereby validating that DN226 peptide can specifically bind to IL-11Rα. DN226 bound to the

receptor with an inhibitory constant (Ki) of 1102 nM, indicating a moderate competition ability.

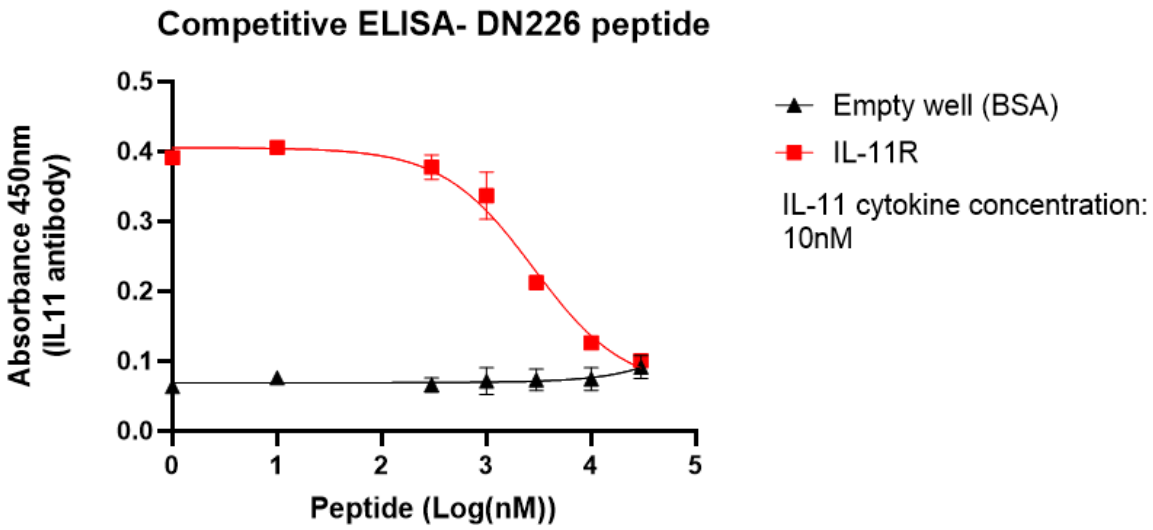

Figure 18. Competitive ELISA demonstrating the competition between DN226 peptide and IL-11 cytokine for binding to IL-11Rα. Absorbance at 450 nm is indicative of anti-hIL-11 antibody binding and is plotted against increasing concentration of DN226 peptide (log (nM)). Absorbance values show a decrease in signal with higher peptide concentrations in the experimental group (red). The negative control group maintained low absorbance values across peptide concentration (black). Error bars indicate standard deviation from replicate measurements. The graph was generated in GraphPad Prism 8.

2.5 Discussion

This study describes a comprehensive workflow, from molecular cloning and mammalian expression of IL-11Rα to the discovery of specific, computationally designed de novo miniprotein inhibitors that target the receptor. The initial phase involved the production of recombinant IL-11Rα through transient transfection of FreeStyle human embryonic kidney (HEK293-F) cells. This cell line is widely used for recombinant protein production due to its highly efficient transfection, rapid growth, and adaptability to serum-free suspension culture (Tan et al., 2021). Using Lipofectamine, a cationic transfection agent (Dalby, 2004), enabled the production of IL-11Rα; however, the yield was low, possibly due to protein aggregation, as evidenced by SDS-PAGE and Western blot analyses (Figures 7 and 8). Nevertheless, it is important to note that the functionally active recombinant protein was successfully produced and validated via the interaction with its natural ligand. However, it showed a lower signal compared to the commercially

available receptor due to the low protein expression yield and a smaller amount of functionally active receptor present in the sample (Figure 9). These issues emphasize the need for further codon optimization and the fine-tuning of expression and purification. Due to these challenges and considering that time is a critical factor in drug development projects, such as this one, commercially available IL-11Rα (validated in ELISA (Figure 10)) was used for downstream assays instead of performing a more time-consuming and costly optimization.

De novo protein design is a powerful approach for creating novel miniproteins with tailored structure and function, offering advantages over not just small molecules, but conventional antibodies as well, including smaller size, improved tissue penetration, lower risk of immunogenicity, and high stability due to its compact structure (Asada et al., 2024; Crook et al., 2020; Kortemme, 2024). The Use of AI can improve de novo protein design by increasing the accuracy of predicting protein structures and interactions, and more efficiently generating potential initial scaffolds (Kortemme, 2024). The phage display biopanning campaign, utilizing the pIII M13 phage system, enabled efficient presentation and selection of a diverse miniprotein library targeting IL-11Rα. This system relies on the creation of a fusion protein that combines the pIII phage coat protein with the protein of interest to be displayed (Jaroszewicz et al., 2022).

During our experiments, four rounds of biopanning yielded robust enrichment of specific binders, demonstrating an effective selection process and the recovery of early candidates (Figure 11). Among enriched clones, two promising miniproteins, DN226 and DN213, emerged as the most promising ones. Both binders exhibited a strong and specific interaction with the target receptor (Figures 12 and 13). Competitive ELISA revealed that DN226 exhibited a higher binding affinity and resilience to IL-11 competition than DN213, both in phage and peptide forms (Figures 14 - 17). At micromolar concentrations, DN226 emerged as a promising scaffold hit for inhibiting IL-11 signaling, showing moderate competition with the IL-11 cytokine (Figure 18). Similarly, Lear et al. (2025) used the pIII phage display to find cyclic peptide inhibitors of IL-11 signaling targeting IL-11 and IL-11Rα. Two disulfide-constrained peptide libraries were biopanned against each target and a counter-target in three rounds, ELISA and FACS showed significant enrichment of binders for IL-11 and IL-11Rα in rounds 2 and 3, with no binding to IL-6R. However, IL-11 couldn't compete with phage clones, indicating peptides bind a

different site than the native ligand. About 1000 clones per target were screened, yielding 209 receptor-binding and 48 unique sequences for the IL-11 campaign; NGS revealed a single consensus, suggesting one binding site. Inhibitors with Ki of 300-400 nM were identified via AlphaLISA, receptor-ligand dimerization inhibition assay, but the promising binder lost activity upon resynthesis (Lear at el. 2025). The broader therapeutic landscape in cytokine signaling, especially IL-6, has shown its essential role in treatment strategies and exemplifies effective receptor-targeted therapies. IL-6 pathway inhibitors focus on either IL-6 or IL-6Rα. Anti-IL-6 drugs like sirukumab, olokizumab, and clazakizumab are in clinical trials but not yet approved, while anti-IL-6R mAbs such as tocilizumab and sarilumab are approved for rheumatoid arthritis (Aletaha et al., 2023). Due to the close functional relationship between IL-11 and IL-6, targeting the receptor might be the most promising approach for developing effective therapies.

De novo computational protein design has been utilized to create proteins with therapeutic potential, such as high-affinity miniprotein binders targeting the SARS-CoV-2 spike protein, which show virus-neutralizing activity in the picomolar range (Cao et al., 2020) Additionally, miniprotein inhibitors targeting oncogenic mutants of BRAF kinase have demonstrated low-micromolar inhibitory activity, suggesting a new starting point in anticancer therapy (Ham et al., 2024). Moreover, de novo designed miniprotein inhibitors targeting two therapeutic targets for autoimmune disease treatment, IL-23R and IL-17, effectively blocked cell signaling in vitro and exhibited high stability (Berger et al., 2024). From a therapeutic perspective, IL-11 signaling plays a crucial role in diseases such as IPF, where it is upregulated and driving pathological fibrotic events (Ng et al., 2019). Targeting IL-11 signaling has been proposed in studies, which show that neutralizing antibodies and siRNA can reduce pro-fibrotic effects (Milara et al., 2022; Ng et al., 2019; Schafer et al., 2017). Given the pathological role of IL-11 and the limited efficacy of current treatments in curing IPF, targeting IL-11 signaling with novel miniprotein inhibitors offers a promising new approach. This study presents a potential new therapeutic approach to treat IPF by inhibiting IL-11 signaling with de novo-designed miniproteins. Innovative computational tools, combined with the use of the phage display system, offer a promising approach for developing new, effective therapeutic agents and achieving improved treatment outcomes.

In upcoming experiments, the project will continue discovering and selecting additional hit molecules and further optimizing them to achieve subnanomolar inhibitors that remain highly selective towards IL-11 receptor. Additionally, a key goal for next year is to evaluate the most promising scaffold hits in an in vivo IPF animal model.

3 General Discussion

This study outlines a comprehensive workflow, from the molecular cloning and mammalian expression of the IL-11Rα to the identification of specific, de novo-designed miniprotein inhibitors targeting this receptor. Biopharmaceutical products, including recombinant proteins, are produced using eukaryotic expression systems. Since the establishment of the HEK293 cell line, various subtypes have gained popularity for the production of recombinant proteins. This cell line is one of the main standards because it is efficiently transfected, produces high levels of protein, grows rapidly, and can be cultured in serum-free suspension for both small- and large-scale production (Tan et al., 2021). During our experiments, the FreeStyle-293-F cell line, derived from the HEK293 cell line, was used to produce of recombinant IL-11Rα. We performed a transient transfection, in which cells were transfected with the pcDNA3.1 plasmid containing the IL-11Rα insert using Lipofectamine, a cationic lipid-based formulation (Dalby, 2004). This method does not involve the integration of foreign DNA into the host genome; therefore, the genetic change is not passed on to the next generation. This type of transfection provides a suitable and straightforward method for producing recombinant proteins on a small scale for several days, after which the foreign DNA is lost as the host cell replicates (Chong et al., 2021; Fus-Kujawa et al., 2021). SDS-PAGE and Western blot results showed that the production yield was low, accompanied by some level of protein aggregation (Figures 7 and 8). However, it is worth noting that the functional validation of the rIL-11Rα confirmed its functional activity to bind the IL-11 cytokine. However, it showed a lower signal compared to the commercially available receptor due to the low protein expression yield and a smaller amount of functionally active receptor present in the sample (Figure 9). Therefore, further construct modifications are needed, such codon optimization and the fine-tuning of expression and purification. As a result, we selected a commercially available IL-11Rα (cIL-11Rα) from AcroBiosystems, for

downstream in vitro assays instead of spending more time optimizing in-house production of rIL-11Rα, which would have required a costly process to obtain enough receptor.

De novo protein design has emerged as a powerful method, allowing for the creation of new proteins with tailored structure and function. Utilizing AI can enhance de novo protein design by enhancing the accuracy of protein structure prediction and generating potential scaffolds more efficiently (Kortemme, 2024). Targeting IL-11Rα with de novo-designed miniproteins could offer an innovative therapeutic strategy, as they possess advantages over conventional monoclonal antibodies, including smaller size, enhanced tissue penetration, reduced immunogenicity, and stability over harsh conditions (Asada et al., 2024; Crook et al., 2020; Roy et al., 2023). The phage display system is a laboratory technique that enables the presentation of a library of proteins, like de novo designed miniproteins, on the surface of bacteriophage virions. This technology is based on genetically modifying phage DNA by inserting a DNA sequence of interest into a gene that encodes one of the phage coat proteins, thereby creating a fusion protein that is displayed on the surface after gene expression. It facilitates the study of protein interactions and the discovery of new protein sequences (Jaroszewicz et al., 2022). Helper phages are necessary as they facilitate the packaging of phagemids containing the gene of interest into phage particles, since they encode the structural proteins required for the packaging process (Jaroszewicz et al., 2022). M13 KO7 helper phage, a modified version of M13 phage, was employed to display de novo proteins on the phage surface for biopanning and in vitro assays.

The results of this work demonstrate the successful application of the phage display system to identify functional, computationally designed de novo miniproteins capable of targeting IL-11 signaling. The workflow involved a powerful combination of computational tools and a classical laboratory experimental approach. The p3 phage monovalent display system effectively presented the de novo designed miniprotein library and enabled the enrichment of cIL-11Rα binders through biopanning. After successfully cloning and transforming NEB 5-alpha cells with the phagemid PAS62 vector containing the miniprotein library with 400 scaffolds, the different scaffolds were expressed on M13 phage surfaces. The results showed that the enrichment factor increased over four rounds of screening, demonstrating the successful selection of specific IL-11R miniprotein binders (Figure 11). Two miniproteins, DN213 and DN226, were identified and isolated

as potential IL-11R binders. Both scaffolds were initially tested while displayed on the phage surface. Phage ELISA results indicated that both miniproteins effectively bind to the cIL-11Rα (Figures 12 and 13). Additionally, a competitive ELISA revealed that both DN226 and DN213 miniproteins specifically target the IL-11 cytokine binding site on the cIL-11Rα. Interestingly, the IL-11 cytokine at a 50 nM concentration was sufficient to achieve full competition with DN213, whereas 250 nM cytokine was required for DN226 in competitive ELISA (Figures 14 and 15). These findings suggest that DN226 exhibits a stronger binding affinity cIL-11Rα compared to DN213 when displayed on the phage surface. Testing miniproteins as peptides further emphasized the functional relevance of these binders. In peptide form, only DN226 demonstrated effective competitive binding to the IL-11 cytokine binding site on cIL-11Rα, highlighting the importance of validating candidates in a non-phage context as well (Figures 16 and 17). Our results demonstrate that at a micromolar concentration, DN226 can effectively bind to the cIL-11Rα with high specificity and moderate competition with IL-11 cytokine, representing a promising hit miniprotein scaffold for inhibiting IL-11 signaling pathways (Figure 18). These findings emphasize the potential of computationally designed de novo miniproteins, which are screened and validated through phage display and ELISA assays, as promising drug candidates.

Lear at el. (2025) utilized the pIII phage display system to identify cyclic peptide inhibitors of IL-11 signaling targeting IL-11 cytokine and IL-11Rα. Two libraries of disulfide-constrained peptides were expressed on phages and biopanned against each target (IL-11, IL-11Rα) and counter-target in three rounds. Both ELISA and fluorescence-activated cell sorting (FACS) demonstrated significant enrichment of phage binders for the targets (IL-11 or IL-11Rα) in rounds 2 and 3, and no binding to IL-6R. However, IL-11 could not compete with phage clones as demonstrated by the phage ELISA and the phage pool result, suggesting that the peptides bound to a different site on the receptor than the native ligand. Approximately 1000 individual phage clones were isolated and screened for each target, yielding 209 unique receptor-binding sequences and 48 unique sequences for IL-11. NGS data showed that only one consensus sequence was identified, indicating a single binding site on the receptor. Inhibitors with Ki of 300-400 nM were identified in AlphaLISA dimerization assay for both IL-11 and IL-11Rα campaign. However, the promising receptor binding hit lost its activity during the resynthesis process and was not advanced any further. The most active IL-11 binder inhibited IL-

11/IL-11Rα dimerization in an AlphaLISA receptor-ligand dimerization inhibition assay with a Ki of 300 nM. Following further structural optimization, it achieved greater activity with a Ki of 180 nM. (Lear et al., 2025). A broader therapeutic landscape in cytokine signaling, particularly IL-6, has demonstrated its significant role in treatment strategies and exemplifies the potential of receptor-targeted therapies. The IL-6 pathway has become a crucial therapeutic target in immune-mediated inflammatory diseases. Efforts to inhibit IL-6 signaling have focused on either directly targeting the IL-6 cytokine or blocking its interaction with IL-6Rα using monoclonal antibodies against IL-6Rα. These anti-IL-6 molecules, including sirukumab, olokizumab, and clazakizumab, have entered clinical trials but have not received approval. In contrast, antibodies that target IL-6R, such as tocilizumab and sarilumab, have been approved for treating rheumatoid arthritis (Aletaha et al., 2023). Given the close functional relationship between IL-11 and IL-6, targeting the receptor may offer the most promising route toward developing effective therapies.

The de novo computational approach has also been employed to design other proteins with therapeutic potential. For instance, high-affinity, de novo designed miniprotein binders were developed to target the interaction between the severe acute respiratory syndrome coronavirus 2 (SARS-CoV-2) spike protein and the human angiotensin-converting enzyme 2 (ACE2) receptor, displaying virus-neutralizing potency in the picomolar range, close to the efficacy of anti-SARS-CoV-2 monoclonal antibodies (Cao et al., 2020). De novo designed hyper-stable IL-2 mimics bind to the IL-2βγc receptor with high affinity and show high therapeutic activity in a mouse model of melanoma and colon cancer. Additionally, structure-based de novo design was used to create miniprotein inhibitors targeting oncogenic BRAF kinase, which showed inhibitory activity at low-micromolar concentrations (Ham et al., 2024). Miniproteins were also designed to target IL-23R and IL-17, successfully inhibiting signaling in vitro, with high stability and antibody-like affinities in the low-picomolar range. Moreover, an orally administered IL-23R-targeting miniprotein was shown to be effective in a mouse model of colitis, exhibiting a slow dissociation rate and high affinity (Berger et al., 2024).

Our findings are crucial, given the pathological role of IL-11 signaling in diseases such as IPF, where IL-11, a key driver of the disease, is highly upregulated. Therefore, IL-11 is an attractive target in drug discovery. Previous research has demonstrated that

various profibrotic growth factors, including TGF-β, induce the release of IL-11, highlighting the pivotal role of IL-11 in fibrotic processes (Ng et al., 2019). Currently, there are two FDA-approved treatments for IPF: nintedanib and pirfenidone. Nintedanib acts by inhibiting receptor tyrosine kinases, while pirfenidone reduces the overexpression of type I collagen and the release of pro-inflammatory cytokines. Although both drugs can slow disease progression, they cannot cure IPF. Consequently, developing new therapeutic strategies targeting novel pathways may lead to effective treatments (C et al., 2020; Mei et al., 2022; Torre et al., 2024). Targeting the IL-11 signaling pathway has been proposed as a potential therapy for fibrotic diseases. Neutralizing IL-11 antibodies, IL-11Rα inhibiting antibodies, and small interfering RNA (siRNA) have been shown to reduce the pro-fibrotic effects of TGF-ß (Schafer et al., 2017). Moreover, anti-IL11 therapy with a neutralizing antibody blocked lung fibroblast activation, reversed lung fibrosis, and decreased lung inflammation in mice (Ng et al., 2019). Additionally, preventing IL-11 from binding to IL-11Rα reduced renal fibrosis and blocked IL-11's downstream effects (Li et al., 2023). Transfection of siRNA-IL-11 in animal models reduced lung and blood fibrocytes, indicating a potential target for treating lung fibrosis (Milara et al., 2024). Furthermore, one monoclonal antibody inhibitor of IL-11 signaling has completed Phase I and Phase IIa clinical trials, while another is currently in Phase I (Pudewell et al., 2025; Schott et al., 2025).

De novo protein design can revolutionize drug discovery process by creating molecules that improve biological functions, enhance therapeutic properties, and reduce side effects faster and with reduced cost. This approach can be applied to cytokines as well as to almost any molecule with a known or predictable 3-dimensional structure (D.-A. Silva et al., 2019). Moreover, de novo protein design offers a wide range of possibilities, enabling the identification of diverse high-affinity binding modes and binders (Cao et al., 2020). The computational design of de novo proteins and the phage display methodology utilized here enable the rapid development of specific binder molecules tailored to therapeutic target molecules, such as IL-11Rα. A starting hit scaffold, like DN226 in this project, serves as a strong foundation for preclinical drug development. Moreover, by leveraging AI, we significantly reduced the cost and shortened the duration of the hit identification stage in the drug discovery funnel, as we achieved hit confirmation roughly six months after the start of the computational design phase. In upcoming experiments, the project will continue to discover and select

additional hit molecules, further optimizing them to achieve subnanomolar inhibitors. Additionally, a key goal for next year is to evaluate the most promising scaffold hits in an in vivo IPF animal model.

4 Conclusions

This study demonstrated an effective method for developing therapeutic agents targeting IL-11 signaling, utilizing advanced de novo protein design and phage display technology. It successfully identified novel miniprotein inhibitors with moderate affinity and favorable specificity for IL-11Rα. The combination of these technologies provides a powerful approach to creating miniprotein scaffolds that compete with the IL-11 cytokine, potentially disrupting pathogenic signaling pathways involved in the progression of fibrotic diseases, such as IPF. The initial phase of this study involved the molecular cloning and mammalian expression of IL-11Rα using the HEK293-F cell line. Despite achieving successful expression, challenges such as low yield and protein aggregation were encountered, indicating the need for further codon optimization and the fine-tuning of expression and purification. This issue prevented the application of the in-house recombinant IL-11Rα (rIL-11Rα) in in vitro assays. Therefore, commercially available IL-11Rα (cIL-11Rα) was employed for downstream assays. However, it is worth noting that the functional validation of the rIL-11Rα confirmed its functional activity to bind the IL-11 cytokine. Through four rounds of biopanning using the pIII M13 phage display system, a diverse miniprotein library containing 400 distinct scaffolds was successfully screened, and specific binders were enriched. Two candidates, DN226 and DN213, emerged as potential IL-11R inhibitors. Binding ELISA confirmed that both miniproteins can bind to their target receptor. Additionally, competitive ELISA showed that DN226 has a higher binding affinity and is more resistant to competition by the IL-11 cytokine than DN213. On the phage surface, DN226 maintained receptor binding even in the presence of 50 nM cytokine, whereas this cytokine concentration nearly completely abolished DN213's binding. This assay also demonstrated that the miniproteins bind to the same site on IL-11Rα as the IL-11 cytokine, indicating a successful structural design. Further validation in peptide form confirmed that DN226 is a more potent binder than DN213, making it the leading candidate for future developments aiming to block the interaction between IL-11 cytokine and its receptor.

Targeting IL-11 signaling is promising due to its key role in fibrotic diseases, such as IPF, where current treatments are limited in their ability to cure the disease. Given the limited options available for current IPF treatment, de novo-designed IL-11 signaling inhibitors offer a promising new possibility as a highly specific targeted therapy. This study presents a promising starting point for the development of therapeutic inhibitors targeting molecular sites with the help of AI-driven computational protein design combined with state-of-the-art "wet lab" techniques and laboratory screening methods. In upcoming experiments, the project will continue to identify and select additional hit molecules, improve their drug-like properties, and evaluate the most promising scaffold hits in an in vivo IPF animal model. In conclusion, combining AI-driven de novo protein design with state-of-the-art wet-lab methods enabled the rapid and cost-effective identification of initial hit molecules with the potential to be refined into drug candidates—surpassing current industry standards.

5 References

Agthe, M., Brügge, J., Garbers, Y., Wandel, M., Kespohl, B., Arnold, P., Flynn, C. M., Lokau, J., Aparicio-Siegmund, S., Bretscher, C., Rose-John, S., Waetzig, G. H., Putoczki, T., Grötzinger, J., & Garbers, C. (2018). Mutations in Craniosynostosis Patients Cause Defective Interleukin-11 Receptor Maturation and Drive Craniosynostosis-like Disease in Mice. *Cell Reports*, *25*(1), 10-18.e5. https://doi.org/10.1016/j.celrep.2018.09.005

Agthe, M., Garbers, Y., Putoczki, T., & Garbers, C. (2017). Interleukin-11 classic but not trans-signaling is essential for fertility in mice. *Placenta*, *57*, 13–16. https://doi.org/10.1016/j.placenta.2017.05.015

Airapetov, M. I., Eresko, S. O., Ignatova, P. D., Lebedev, A. A., Bychkov, E. R., & Shabanov, P. D. (2023). Interleukin-11 in Pathologies of the Nervous System. *Molecular Biology*, *57*(1), 1–6. https://doi.org/10.1134/S0026893323010028

Akdis, M., Burgler, S., Crameri, R., Eiwegger, T., Fujita, H., Gomez, E., Klunker, S., Meyer, N., O'Mahony, L., Palomares, O., Rhyner, C., Quaked, N., Schaffartzik, A., Van De Veen, W., Zeller, S., Zimmermann, M., & Akdis, C. A. (2011). Interleukins, from 1 to 37, and interferon-γ: Receptors, functions, and roles in diseases. *Journal of Allergy and Clinical Immunology*, *127*(3), 701-721.e70. https://doi.org/10.1016/j.jaci.2010.11.050

Aletaha, D., Kerschbaumer, A., Kastrati, K., Dejaco, C., Dougados, M., McInnes, I. B., Sattar, N., Stamm, T. A., Takeuchi, T., Trauner, M., van der Heijde, D., Voshaar, M., Winthrop, K. L., Ravelli, A., Betteridge, N., Burmester, G.-R. R., Bijlsma, J. W., Bykerk, V., Caporali, R., … Smolen, J. S. (2023). Consensus statement on blocking interleukin-6 receptor and interleukin-6 in inflammatory conditions: an update. *Annals of the Rheumatic Diseases*, *82*(6), 773–787. https://doi.org/10.1136/ard-2022-222784

Asada, N., Krebs, C. F., & Panzer, U. (2024). Miniproteins may have a big impact: new therapeutics for autoimmune diseases and beyond. *Signal Transduction and Targeted Therapy*, *9*(1), 298. https://doi.org/10.1038/s41392-024-02010-z

Ayaub, E. A., Dubey, A., Imani, J., Botelho, F., Kolb, M. R. J., Richards, C. D., & Ask, K. (2017). Overexpression of OSM and IL-6 impacts the polarization of pro-

fibrotic macrophages and the development of bleomycin-induced lung fibrosis. *Scientific Reports*, *7*(1), 13281. https://doi.org/10.1038/s41598-017-13511-z

Baker, E. G., Bartlett, G. J., Porter Goff, K. L., & Woolfson, D. N. (2017). Miniprotein Design: Past, Present, and Prospects. *Accounts of Chemical Research*, *50*(9), 2085–2092. https://doi.org/10.1021/acs.accounts.7b00186

Barratt, S., Creamer, A., Hayton, C., & Chaudhuri, N. (2018). Idiopathic Pulmonary Fibrosis (IPF): An Overview. *Journal of Clinical Medicine*, *7*(8), 201. https://doi.org/10.3390/jcm7080201

Berger, S., Seeger, F., Yu, T.-Y., Aydin, M., Yang, H., Rosenblum, D., Guenin-Macé, L., Glassman, C., Arguinchona, L., Sniezek, C., Blackstone, A., Carter, L., Ravichandran, R., Ahlrichs, M., Murphy, M., Pultz, I. S., Kang, A., Bera, A. K., Stewart, L., … Baker, D. (2024). Preclinical proof of principle for orally delivered Th17 antagonist miniproteins. *Cell*, *187*(16), 4305-4317.e18. https://doi.org/10.1016/j.cell.2024.05.052

Bravo, J. (1998). Crystal structure of a cytokine-binding region of gp130. *The EMBO Journal*, *17*(6), 1665–1674. https://doi.org/10.1093/emboj/17.6.1665

C, L., A, C., L, V., L, B., d'Alessandro M, P, C., G, S., F, D., & E, B. (2020). Common molecular pathways targeted by nintedanib in cancer and IPF: A bioinformatic study. *Pulmonary Pharmacology & Therapeutics*, *64*, 101941. https://doi.org/10.1016/j.pupt.2020.101941

Camelo, A., Dunmore, R., Sleeman, M. A., & Clarke, D. L. (2014). The epithelium in idiopathic pulmonary fibrosis: breaking the barrier. *Frontiers in Pharmacology*, *4*. https://doi.org/10.3389/fphar.2013.00173

Cao, L., Coventry, B., Goreshnik, I., Huang, B., Sheffler, W., Park, J. S., Jude, K. M., Marković, I., Kadam, R. U., Verschueren, K. H. G., Verstraete, K., Walsh, S. T. R., Bennett, N., Phal, A., Yang, A., Kozodoy, L., DeWitt, M., Picton, L., Miller, L., … Baker, D. (2022). Design of protein-binding proteins from the target structure alone. *Nature*, *605*(7910), 551–560. https://doi.org/10.1038/s41586-022-04654-9

Cao, L., Goreshnik, I., Coventry, B., Case, J. B., Miller, L., Kozodoy, L., Chen, R. E., Carter, L., Walls, A. C., Park, Y.-J., Strauch, E.-M., Stewart, L., Diamond, M. S.,

Veesler, D., & Baker, D. (2020). De novo design of picomolar SARS-CoV-2 miniprotein inhibitors. *Science*, *370*(6515), 426–431. https://doi.org/10.1126/science.abd9909

Chevalier, A., Silva, D.-A., Rocklin, G. J., Hicks, D. R., Vergara, R., Murapa, P., Bernard, S. M., Zhang, L., Lam, K.-H., Yao, G., Bahl, C. D., Miyashita, S.-I., Goreshnik, I., Fuller, J. T., Koday, M. T., Jenkins, C. M., Colvin, T., Carter, L., Bohn, A., … Baker, D. (2017). Massively parallel de novo protein design for targeted therapeutics. *Nature*, *550*(7674), 74–79. https://doi.org/10.1038/nature23912

Chong, Z. X., Yeap, S. K., & Ho, W. Y. (2021). Transfection types, methods and strategies: a technical review. *PeerJ*, *9*, e11165. https://doi.org/10.7717/peerj.11165

Chow, D., Brevnova, L., He, X., Martick, M. M., Bankovich, A., & Garcia, K. C. (2002). A structural template for gp130-cytokine signaling assemblies. *Biochimica et Biophysica Acta (BBA) - Molecular Cell Research*, *1592*(3), 225–235. https://doi.org/10.1016/S0167-4889(02)00317-8

Coles, B., Fielding, C. A., Rose-John, S., Scheller, J., Jones, S. A., & O'Donnell, V. B. (2007). Classic Interleukin-6 Receptor Signaling and Interleukin-6 trans-Signaling Differentially Control Angiotensin II-Dependent Hypertension, Cardiac Signal Transducer and Activator of Transcription-3 Activation, and Vascular Hypertrophy in Vivo. *The American Journal of Pathology*, *171*(1), 315–325. https://doi.org/10.2353/ajpath.2007.061078

Collard, H. R., King, T. E., Bartelson, B. B., Vourlekis, J. S., Schwarz, M. I., & Brown, K. K. (2003). Changes in Clinical and Physiologic Variables Predict Survival in Idiopathic Pulmonary Fibrosis. *American Journal of Respiratory and Critical Care Medicine*, *168*(5), 538–542. https://doi.org/10.1164/rccm.200211-1311OC

Cork, B. A., Li, T. C., Warren, M. A., & Laird, S. M. (2001). Interleukin-11 (IL-11) in human endometrium: expression throughout the menstrual cycle and the effects of cytokines on endometrial IL-11 production in vitro. *Journal of Reproductive Immunology*, *50*(1), 3–17. https://doi.org/10.1016/S0165-0378(00)00089-9

Crook, Z. R., Nairn, N. W., & Olson, J. M. (2020). Miniproteins as a Powerful Modality in Drug Development. *Trends in Biochemical Sciences*, *45*(4), 332–346. https://doi.org/10.1016/j.tibs.2019.12.008

Curfs, J. H. A. J., Meis, J. F. G. M., & Hoogkamp-Korstanje, J. A. A. (1997). *A Primer on Cytokines: Sources, Receptors, Effects, and Inducers* (Vol. 10, Issue 4). https://journals.asm.org/journal/cmr

Curtis, D. J., Hilton, D. J., Roberts, B., Murray, L., Nicola, N., & Begley, C. G. (1997). Recombinant soluble interleukin-11 (IL-11) receptor alpha-chain can act as an IL-11 antagonist. *Blood*, *90*(11), 4403–4412.

Czupryn, M. J., McCoy, J. M., & Scoble, H. A. (1995). Structure-Function Relationships in Human Interleukin-11. *Journal of Biological Chemistry*, *270*(2), 978–985. https://doi.org/10.1074/jbc.270.2.978

Dalby, B. (2004). Advanced transfection with Lipofectamine 2000 reagent: primary neurons, siRNA, and high-throughput applications. *Methods*, *33*(2), 95–103. https://doi.org/10.1016/j.ymeth.2003.11.023

Dayer, J.-M., & Choy, E. (2010). Therapeutic targets in rheumatoid arthritis: the interleukin-6 receptor. *Rheumatology*, *49*(1), 15–24. https://doi.org/10.1093/rheumatology/kep329

Dinarello, C. A. (2007). Historical insights into cytokines. *European Journal of Immunology*, *37*(S1), S34–S45. https://doi.org/10.1002/eji.200737772

Du, X., & Williams, D. A. (1997). Interleukin-11: Review of Molecular, Cell Biology, and Clinical Use. *Blood*, *89*(11), 3897–3908. https://doi.org/10.1182/blood.V89.11.3897

Elias, J. A., Zheng, T., Whiting, N. L., Trow, T. K., Merrill, W. W., Zitnik, R., Ray, P., & Alderman, E. M. (1994). IL-1 and transforming growth factor-beta regulation of fibroblast-derived IL-11. *The Journal of Immunology*, *152*(5), 2421–2429. https://doi.org/10.4049/jimmunol.152.5.2421

Fearon, U., Mullan, R., Markham, T., Connolly, M., Sullivan, S., Poole, A. R., FitzGerald, O., Bresnihan, B., & Veale, D. J. (2006). Oncostatin M induces angiogenesis and cartilage degradation in rheumatoid arthritis synovial tissue and human cartilage cocultures. *Arthritis & Rheumatism*, *54*(10), 3152–3162. https://doi.org/10.1002/art.22161

Fernandez, I. E., & Eickelberg, O. (2012). The Impact of TGF-β on Lung Fibrosis. *Proceedings of the American Thoracic Society*, *9*(3), 111–116. https://doi.org/10.1513/pats.201203-023AW

Freire, E., & Murphy, K. P. (1991). Molecular basis of co-operativity in protein folding. *Journal of Molecular Biology*, *222*(3), 687–698. https://doi.org/10.1016/0022-2836(91)90505-Z

Fung, K. Y., Louis, C., Metcalfe, R. D., Kosasih, C. C., Wicks, I. P., Griffin, M. D. W., & Putoczki, T. L. (2022). Emerging roles for IL-11 in inflammatory diseases. *Cytokine*, *149*, 155750. https://doi.org/10.1016/j.cyto.2021.155750

Fus-Kujawa, A., Prus, P., Bajdak-Rusinek, K., Teper, P., Gawron, K., Kowalczuk, A., & Sieron, A. L. (2021). An Overview of Methods and Tools for Transfection of Eukaryotic Cells in vitro. *Frontiers in Bioengineering and Biotechnology*, *9*. https://doi.org/10.3389/fbioe.2021.701031

Gardner, S., Jin, Y., Fyfe, P. K., Voisin, T. B., Bellón, J. S., Pohler, E., Piehler, J., Moraga, I., & Bubeck, D. (2024). Structural insights into IL-11-mediated signalling and human IL6ST variant-associated immunodeficiency. *Nature Communications*, *15*(1), 2071. https://doi.org/10.1038/s41467-024-46235-6

Geng, Y., Liu, X., Liang, J., Habiel, D. M., Vrishika, K., Coelho, A. L., Deng, N., Xie, T., Wang, Y., Liu, N., Huang, G., Kurkciyan, A., Liu, Z., Tang, J., Hogaboam, C. M., Jiang, D., & Noble, P. W. (2019). PD-L1 on invasive fibroblasts drives fibrosis in a humanized model of idiopathic pulmonary fibrosis. *JCI Insight*. https://doi.org/10.1172/jci.insight.125326

George, P. M., Patterson, C. M., Reed, A. K., & Thillai, M. (2019). Lung transplantation for idiopathic pulmonary fibrosis. *The Lancet Respiratory Medicine*, *7*(3), 271–282. https://doi.org/10.1016/S2213-2600(18)30502-2

Gerber, D. E. (2008). Targeted therapies: a new generation of cancer treatments. *American Family Physician*, *77*(3), 311–319.

Glass, D. S., Grossfeld, D., Renna, H. A., Agarwala, P., Spiegler, P., DeLeon, J., & Reiss, A. B. (2022). Idiopathic pulmonary fibrosis: Current and future treatment. *The Clinical Respiratory Journal*, *16*(2), 84–96. https://doi.org/10.1111/crj.13466

Goodman, R. B., Pugin, J., Lee, J. S., & Matthay, M. A. (2003). Cytokine-mediated inflammation in acute lung injury. *Cytokine & Growth Factor Reviews*, *14*(6), 523–535. https://doi.org/10.1016/S1359-6101(03)00059-5

Grinnell, F. (2003). Fibroblast biology in three-dimensional collagen matrices. *Trends in Cell Biology*, *13*(5), 264–269. https://doi.org/10.1016/S0962-8924(03)00057-6

Ham, J. M., Kim, M., Kim, T., Ryu, S. E., & Park, H. (2024). Structure-Based De Novo Design for the Discovery of Miniprotein Inhibitors Targeting Oncogenic Mutant BRAF. *International Journal of Molecular Sciences*, *25*(10), 5535. https://doi.org/10.3390/ijms25105535

Han, Y., Gao, H., Gan, X., Liu, J., Bao, C., & He, C. (2024). Roles of IL-11 in the regulation of bone metabolism. *Frontiers in Endocrinology*, *14*. https://doi.org/10.3389/fendo.2023.1290130

Heinrich, P. C., Behrmann, I., Haan, S., Hermanns, H. M., Müller-Newen, G., & Schaper, F. (2003). Principles of interleukin (IL)-6-type cytokine signalling and its regulation. *Biochemical Journal*, *374*(1), 1–20. https://doi.org/10.1042/bj20030407

Hilton, D. J., Watowich, S. S., Katz, L., & Lodish, H. F. (1996). Saturation Mutagenesis of the WSXWS Motif of the Erythropoietin Receptor. *Journal of Biological Chemistry*, *271*(9), 4699–4708. https://doi.org/10.1074/jbc.271.9.4699

Hirano, T., Nakajima, K., & Hibi, M. (1997). Signaling mechanisms through gp130: A model of the cytokine system. *Cytokine & Growth Factor Reviews*, *8*(4), 241–252. https://doi.org/10.1016/S1359-6101(98)80005-1

Huang, G., Yu, L., Cooper, L. J. N., Hollomon, M., Huls, H., & Kleinerman, E. S. (2012). Genetically Modified T cells Targeting Interleukin-11 Receptor α-Chain Kill Human Osteosarcoma Cells and Induce the Regression of Established Osteosarcoma Lung Metastases. *Cancer Research*, *72*(1), 271–281. https://doi.org/10.1158/0008-5472.CAN-11-2778

Huang, P.-S., Boyken, S. E., & Baker, D. (2016). The coming of age of de novo protein design. *Nature*, *537*(7620), 320–327. https://doi.org/10.1038/nature19946

Iqbal, J., Sun, L., & Zaidi, M. (2010). Complexity in signal transduction. *Annals of the New York Academy of Sciences*, *1192*(1), 238–244. https://doi.org/10.1111/j.1749-6632.2010.05388.x

Jaroszewicz, W., Morcinek-Orłowska, J., Pierzynowska, K., Gaffke, L., & Węgrzyn, G. (2022). Phage display and other peptide display technologies. *FEMS Microbiology Reviews*, *46*(2). https://doi.org/10.1093/femsre/fuab052

Jones, S. A., Horiuchi, S., Topley, N., Yamamoto, N., & Fuller, G. M. (2001). The soluble interleukin 6 receptor: mechanisms of production and implications in disease. *The FASEB Journal*, *15*(1), 43–58. https://doi.org/10.1096/fj.99-1003rev

Kaminska, B. (2005). MAPK signalling pathways as molecular targets for anti-inflammatory therapy—from molecular mechanisms to therapeutic benefits. *Biochimica et Biophysica Acta (BBA) - Proteins and Proteomics*, *1754*(1–2), 253–262. https://doi.org/10.1016/j.bbapap.2005.08.017

Kany, S., Vollrath, J. T., & Relja, B. (2019). Cytokines in Inflammatory Disease. *International Journal of Molecular Sciences*, *20*(23), 6008. https://doi.org/10.3390/ijms20236008

King, T. E., Pardo, A., & Selman, M. (2011). Idiopathic pulmonary fibrosis. *The Lancet*, *378*(9807), 1949–1961. https://doi.org/10.1016/S0140-6736(11)60052-4

Kis, K., Liu, X., & Hagood, J. S. (2011). Myofibroblast differentiation and survival in fibrotic disease. *Expert Reviews in Molecular Medicine*, *13*, e27. https://doi.org/10.1017/S1462399411001967

Kohrs, L., Buettner, F. F. R., Lokau, J., & Garbers, C. (2025). The biology of interleukin-6 family cytokines is regulated by glycosylation. *Biochemical Journal*, *482*(10), 535–551. https://doi.org/10.1042/BCJ20240769

Kortekaas, R. K., Burgess, J. K., van Orsoy, R., Lamb, D., Webster, M., & Gosens, R. (2021). Therapeutic Targeting of IL-11 for Chronic Lung Disease. *Trends in Pharmacological Sciences*, *42*(5), 354–366. https://doi.org/10.1016/j.tips.2021.01.007

Kortemme, T. (2024). De novo protein design—From new structures to programmable functions. *Cell*, *187*(3), 526–544. https://doi.org/10.1016/j.cell.2023.12.028

Kumari, N., Dwarakanath, B. S., Das, A., & Bhatt, A. N. (2016). Role of interleukin-6 in cancer progression and therapeutic resistance. *Tumor Biology*, *37*(9), 11553–11572. https://doi.org/10.1007/s13277-016-5098-7

Kurth, I., Horsten, U., Pflanz, S., Timmermann, A., Küster, A., Dahmen, H., Tacken, I., Heinrich, P. C., & Müller-Newen, G. (2000). Importance of the Membrane-Proximal Extracellular Domains for Activation of the Signal Transducer Glycoprotein 130. *The Journal of Immunology*, *164*(1), 273–282. https://doi.org/10.4049/jimmunol.164.1.273

Lear, S., Tafi, R., Di Biasio, V. A., Halkowycz, P., Kamran, R., Miura, J., Gibson, T. S., Li, J., Bleck, B., Dall'Armi, C., Demartis, A., & Henninot, A. (2025). De novo discovery of cyclic peptide inhibitors of IL-11 signaling. *Bioorganic & Medicinal Chemistry*, *119*, 118017. https://doi.org/10.1016/j.bmc.2024.118017

Leonard, W. J., & Lin, J.-X. (2000). Cytokine receptor signaling pathways. *Journal of Allergy and Clinical Immunology*, *105*(5), 877–888. https://doi.org/10.1067/mai.2000.106899

Liu, C., Chu, D., Kalantar-Zadeh, K., George, J., Young, H. A., & Liu, G. (2021). Cytokines: From Clinical Significance to Quantification. *Advanced Science*, *8*(15). https://doi.org/10.1002/advs.202004433

Lokau, J., Kespohl, B., Kirschke, S., & Garbers, C. (2022). The role of proteolysis in interleukin-11 signaling. *Biochimica et Biophysica Acta (BBA) - Molecular Cell Research*, *1869*(1), 119135. https://doi.org/10.1016/j.bbamcr.2021.119135

Lokau, J., Nitz, R., Agthe, M., Monhasery, N., Aparicio-Siegmund, S., Schumacher, N., Wolf, J., Möller-Hackbarth, K., Waetzig, G. H., Grötzinger, J., Müller-Newen, G., Rose-John, S., Scheller, J., & Garbers, C. (2016). Proteolytic Cleavage Governs Interleukin-11 Trans-signaling. *Cell Reports*, *14*(7), 1761–1773. https://doi.org/10.1016/j.celrep.2016.01.053

Maher, T. M., & Strek, M. E. (2019). Antifibrotic therapy for idiopathic pulmonary fibrosis: time to treat. *Respiratory Research*, *20*(1), 205. https://doi.org/10.1186/s12931-019-1161-4

Malhotra, P., & Udgaonkar, J. B. (2016). How cooperative are protein folding and unfolding transitions? *Protein Science*, *25*(11), 1924–1941. https://doi.org/10.1002/pro.3015

Martin, L., & Vita, C. (2000). Engineering Novel Bioactive Mini-Proteins from Small Size Natural and De Novo Designed Scaffolds. *Current Protein & Peptide Science*, *1*(4), 403–430. https://doi.org/10.2174/1389203003381306

Medzhitov, R., & Janeway, C. A. (1997). Innate immunity: impact on the adaptive immune response. *Current Opinion in Immunology*, *9*(1), 4–9. https://doi.org/10.1016/S0952-7915(97)80152-5

Mei, Q., Liu, Z., Zuo, H., Yang, Z., & Qu, J. (2022). Idiopathic Pulmonary Fibrosis: An Update on Pathogenesis. *Frontiers in Pharmacology*, *12*. https://doi.org/10.3389/fphar.2021.797292

Meltzer, E. B., & Noble, P. W. (2008). Idiopathic pulmonary fibrosis. *Orphanet Journal of Rare Diseases*, *3*(1), 8. https://doi.org/10.1186/1750-1172-3-8

Metcalfe, R. D., Aizel, K., Zlatic, C. O., Nguyen, P. M., Morton, C. J., Lio, D. S.-S., Cheng, H.-C., Dobson, R. C. J., Parker, M. W., Gooley, P. R., Putoczki, T. L., & Griffin, M. D. W. (2020). The structure of the extracellular domains of human interleukin 11α receptor reveals mechanisms of cytokine engagement. *Journal of Biological Chemistry*, *295*(24), 8285–8301. https://doi.org/10.1074/jbc.RA119.012351

Metcalfe, R. D., Hanssen, E., Fung, K. Y., Aizel, K., Kosasih, C. C., Zlatic, C. O., Doughty, L., Morton, C. J., Leis, A. P., Parker, M. W., Gooley, P. R., Putoczki, T. L., & Griffin, M. D. W. (2023). Structures of the interleukin 11 signalling complex reveal gp130 dynamics and the inhibitory mechanism of a cytokine variant. *Nature Communications*, *14*(1), 7543. https://doi.org/10.1038/s41467-023-42754-w

Metcalfe, R. D., Putoczki, T. L., & Griffin, M. D. W. (2020). Structural Understanding of Interleukin 6 Family Cytokine Signaling and Targeted Therapies: Focus on Interleukin 11. *Frontiers in Immunology*, *11*. https://doi.org/10.3389/fimmu.2020.01424

Milara, J., Roger, I., Montero, P., Artigues, E., Escrivá, J., & Cortijo, J. (2022). IL-11 system participates in pulmonary artery remodeling and hypertension in pulmonary fibrosis. *Respiratory Research*, *23*(1), 313. https://doi.org/10.1186/s12931-022-02241-0

Morris, R., Kershaw, N. J., & Babon, J. J. (2018). The molecular details of cytokine signaling via the JAK/STAT pathway. *Protein Science*, *27*(12), 1984–2009. https://doi.org/10.1002/pro.3519

Moss, B. J., Ryter, S. W., & Rosas, I. O. (2022). Pathogenic Mechanisms Underlying Idiopathic Pulmonary Fibrosis. *Annual Review of Pathology: Mechanisms of Disease*, *17*(1), 515–546. https://doi.org/10.1146/annurev-pathol-042320-030240

Nandurkar, H. H., Robb, L., Tarlinton, D., Barnett, L., Köntgen, F., & Begley, C. G. (1997). Adult mice with targeted mutation of the interleukin-11 receptor (IL11Ra) display normal hematopoiesis. *Blood*, *90*(6), 2148–2159.

Neben, S., & Turner, K. (1996). The biology of interleukin 11. *STEM CELLS*, *11*(S2), 156–162. https://doi.org/10.1002/stem.5530110825

Ng, B., Cook, S. A., & Schafer, S. (2020). Interleukin-11 signaling underlies fibrosis, parenchymal dysfunction, and chronic inflammation of the airway. *Experimental & Molecular Medicine*, *52*(12), 1871–1878. https://doi.org/10.1038/s12276-020-00531-5

Ng, B., Dong, J., D'Agostino, G., Viswanathan, S., Widjaja, A. A., Lim, W.-W., Ko, N. S. J., Tan, J., Chothani, S. P., Huang, B., Xie, C., Pua, C. J., Chacko, A.-M., Guimarães-Camboa, N., Evans, S. M., Byrne, A. J., Maher, T. M., Liang, J., Jiang, D., … Cook, S. A. (2019). Interleukin-11 is a therapeutic target in idiopathic pulmonary fibrosis. *Science Translational Medicine*, *11*(511). https://doi.org/10.1126/scitranslmed.aaw1237

Ng, B., Dong, J., Viswanathan, S., D'Agostino, G., Widjaja, A. A., Lim, W.-W., Ko, N. SJ., Tan, J., Chothani, S. P., Huang, B., Xie, C., Chacko, A.-M., Guimarães-Camboa, N., Evans, S. M., Byrne, A. J., Maher, T. M., Liang, J., Noble, P. W., Schafer, S., & Cook, S. A. (2018). *IL-11 is a therapeutic target in idiopathic pulmonary fibrosis*. https://doi.org/10.1101/336537

Ng, B., Dong, J., Viswanathan, S., Widjaja, A. A., Paleja, B. S., Adami, E., Ko, N. S. J., Wang, M., Lim, S., Tan, J., Chothani, S. P., Albani, S., Schafer, S., & Cook, S.

A. (2020). Fibroblast-specific IL11 signaling drives chronic inflammation in murine fibrotic lung disease. *The FASEB Journal*, *34*(9), 11802–11815. https://doi.org/10.1096/fj.202001045RR

Ng, B., Widjaja, A. A., Viswanathan, S., Dong, J., Chothani, S. P., Lim, S., Shekeran, S. G., Tan, J., McGregor, N. E., Walker, E. C., Sims, N. A., Schafer, S., & Cook, S. A. (2021). Similarities and differences between IL11 and IL11RA1 knockout mice for lung fibro-inflammation, fertility and craniosynostosis. *Scientific Reports*, *11*(1), 14088. https://doi.org/10.1038/s41598-021-93623-9

Nguyen, P. M., Abdirahman, S. M., & Putoczki, T. L. (2019). Emerging roles for Interleukin-11 in disease. *Growth Factors*, *37*(1–2), 1–11. https://doi.org/10.1080/08977194.2019.1620227

Nieminen, P., Morgan, N. V., Fenwick, A. L., Parmanen, S., Veistinen, L., Mikkola, M. L., van der Spek, P. J., Giraud, A., Judd, L., Arte, S., Brueton, L. A., Wall, S. A., Mathijssen, I. M. J., Maher, E. R., Wilkie, A. O. M., Kreiborg, S., & Thesleff, I. (2011). Inactivation of IL11 Signaling Causes Craniosynostosis, Delayed Tooth Eruption, and Supernumerary Teeth. *The American Journal of Human Genetics*, *89*(1), 67–81. https://doi.org/10.1016/j.ajhg.2011.05.024

Nishina, T., Deguchi, Y., Ohshima, D., Takeda, W., Ohtsuka, M., Shichino, S., Ueha, S., Yamazaki, S., Kawauchi, M., Nakamura, E., Nishiyama, C., Kojima, Y., Adachi-Akahane, S., Hasegawa, M., Nakayama, M., Oshima, M., Yagita, H., Shibuya, K., Mikami, T., … Nakano, H. (2021). Interleukin-11-expressing fibroblasts have a unique gene signature correlated with poor prognosis of colorectal cancer. *Nature Communications*, *12*(1), 2281. https://doi.org/10.1038/s41467-021-22450-3

Nobel Prize. (2024). *David Baker-Facts-2024*. <https://Www.Nobelprize.Org/Prizes/Chemistry/2024/Baker/Facts/>.

O'Reilly, S. (2023). Interleukin-11 and its eminent role in tissue fibrosis: a possible therapeutic target. *Clinical and Experimental Immunology*, *214*(2), 154–161. https://doi.org/10.1093/cei/uxad108

Paiva, S. (2024). Protein prediction takes the prize. *Nature Chemistry*, *16*(12), 1938–1938. https://doi.org/10.1038/s41557-024-01699-3

Paul, S. R., Bennett, F., Calvetti, J. A., Kelleher, K., Wood, C. R., O'Hara, R. M., Leary, A. C., Sibley, B., Clark, S. C., & Williams, D. A. (1990). Molecular cloning of a cDNA encoding interleukin 11, a stromal cell-derived lymphopoietic and hematopoietic cytokine. *Proceedings of the National Academy of Sciences*, *87*(19), 7512–7516. https://doi.org/10.1073/pnas.87.19.7512

Plikus, M. V., Wang, X., Sinha, S., Forte, E., Thompson, S. M., Herzog, E. L., Driskell, R. R., Rosenthal, N., Biernaskie, J., & Horsley, V. (2021). Fibroblasts: Origins, definitions, and functions in health and disease. *Cell*, *184*(15), 3852–3872. https://doi.org/10.1016/j.cell.2021.06.024

Popov, Y., & Schuppan, D. (2009). Targeting Liver Fibrosis. *Hepatology*, *50*(4), 1294–1306. https://doi.org/10.1002/hep.23123

Putoczki, T. L., Dobson, R. C. J., & Griffin, M. D. W. (2014). The structure of human interleukin-11 reveals receptor-binding site features and structural differences from interleukin-6. *Acta Crystallographica Section D Biological Crystallography*, *70*(9), 2277–2285. https://doi.org/10.1107/S1399004714012267

Putoczki, T. L., Thiem, S., Loving, A., Busuttil, R. A., Wilson, N. J., Ziegler, P. K., Nguyen, P. M., Preaudet, A., Farid, R., Edwards, K. M., Boglev, Y., Luwor, R. B., Jarnicki, A., Horst, D., Boussioutas, A., Heath, J. K., Sieber, O. M., Pleines, I., Kile, B. T., … Ernst, M. (2013). Interleukin-11 Is the Dominant IL-6 Family Cytokine during Gastrointestinal Tumorigenesis and Can Be Targeted Therapeutically. *Cancer Cell*, *24*(2), 257–271. https://doi.org/10.1016/j.ccr.2013.06.017

Raghu, G., Collard, H. R., Egan, J. J., Martinez, F. J., Behr, J., Brown, K. K., Colby, T. V., Cordier, J.-F., Flaherty, K. R., Lasky, J. A., Lynch, D. A., Ryu, J. H., Swigris, J. J., Wells, A. U., Ancochea, J., Bouros, D., Carvalho, C., Costabel, U., Ebina, M., … Schünemann, H. J. (2011). An Official ATS/ERS/JRS/ALAT Statement: Idiopathic Pulmonary Fibrosis: Evidence-based Guidelines for Diagnosis and Management. *American Journal of Respiratory and Critical Care Medicine*, *183*(6), 788–824. https://doi.org/10.1164/rccm.2009-040GL

Reeh, H., Rudolph, N., Billing, U., Christen, H., Streif, S., Bullinger, E., Schliemann-Bullinger, M., Findeisen, R., Schaper, F., Huber, H. J., & Dittrich, A. (2019). Response to IL-6 trans- and IL-6 classic signalling is determined by the ratio of the IL-6

receptor α to gp130 expression: fusing experimental insights and dynamic modelling. *Cell Communication and Signaling*, *17*(1), 46. https://doi.org/10.1186/s12964-019-0356-0

Richeldi, L., Collard, H. R., & Jones, M. G. (2017). Idiopathic pulmonary fibrosis. *The Lancet*, *389*(10082), 1941–1952. https://doi.org/10.1016/S0140-6736(17)30866-8

Rose-John, S. (2018). Interleukin-6 Family Cytokines. *Cold Spring Harbor Perspectives in Biology*, *10*(2), a028415. https://doi.org/10.1101/cshperspect.a028415

Roy, A., Shi, L., Chang, A., Dong, X., Fernandez, A., Kraft, J. C., Li, J., Le, V. Q., Winegar, R. V., Cherf, G. M., Slocum, D., Poulson, P. D., Casper, G. E., Vallecillo-Zúniga, M. L., Valdoz, J. C., Miranda, M. C., Bai, H., Kipnis, Y., Olshefsky, A., … Baker, D. (2023). De novo design of highly selective miniprotein inhibitors of integrins αvβ6 and αvβ8. *Nature Communications*, *14*(1), 5660. https://doi.org/10.1038/s41467-023-41272-z

Rozwarski, D. A., Gronenborn, A. M., Clore, G. M., Bazan, J. F., Bohm, A., Wlodawer, A., Hatada, M., & Karplus, P. A. (1994). Structural comparisons among the short-chain helical cytokines. *Structure*, *2*(3), 159–173. https://doi.org/10.1016/S0969-2126(00)00018-6

Santos, M. D., Yasuike, M., Kondo, H., Hirono, I., & Aoki, T. (2008). Teleostean IL11b exhibits complementing function to IL11a and expansive involvement in antibacterial and antiviral responses. *Molecular Immunology*, *45*(12), 3494–3501. https://doi.org/10.1016/j.molimm.2008.02.004

Schafer, S., Viswanathan, S., Widjaja, A. A., Lim, W.-W., Moreno-Moral, A., DeLaughter, D. M., Ng, B., Patone, G., Chow, K., Khin, E., Tan, J., Chothani, S. P., Ye, L., Rackham, O. J. L., Ko, N. S. J., Sahib, N. E., Pua, C. J., Zhen, N. T. G., Xie, C., … Cook, S. A. (2017). IL-11 is a crucial determinant of cardiovascular fibrosis. *Nature*, *552*(7683), 110–115. https://doi.org/10.1038/nature24676

Scheller, J., Chalaris, A., Schmidt-Arras, D., & Rose-John, S. (2011). The pro- and anti-inflammatory properties of the cytokine interleukin-6. *Biochimica et Biophysica Acta (BBA) - Molecular Cell Research*, *1813*(5), 878–888. https://doi.org/10.1016/j.bbamcr.2011.01.034

Schiller, H. B., Montoro, D. T., Simon, L. M., Rawlins, E. L., Meyer, K. B., Strunz, M., Vieira Braga, F. A., Timens, W., Koppelman, G. H., Budinger, G. R. S., Burgess, J. K., Waghray, A., van den Berge, M., Theis, F. J., Regev, A., Kaminski, N., Rajagopal, J., Teichmann, S. A., Misharin, A. V., & Nawijn, M. C. (2019). The Human Lung Cell Atlas: A High-Resolution Reference Map of the Human Lung in Health and Disease. *American Journal of Respiratory Cell and Molecular Biology*, *61*(1), 31–41. https://doi.org/10.1165/rcmb.2018-0416TR

Silva, D.-A., Yu, S., Ulge, U. Y., Spangler, J. B., Jude, K. M., Labão-Almeida, C., Ali, L. R., Quijano-Rubio, A., Ruterbusch, M., Leung, I., Biary, T., Crowley, S. J., Marcos, E., Walkey, C. D., Weitzner, B. D., Pardo-Avila, F., Castellanos, J., Carter, L., Stewart, L., … Baker, D. (2019). De novo design of potent and selective mimics of IL-2 and IL-15. *Nature*, *565*(7738), 186–191. https://doi.org/10.1038/s41586-018-0830-7

Silva, W. A., Covas, D. T., Panepucci, R. A., Proto-Siqueira, R., Siufi, J. L. C., Zanette, D. L., Santos, A. R. D., & Zago, M. A. (2003). The Profile of Gene Expression of Human Marrow Mesenchymal Stem Cells. *STEM CELLS*, *21*(6), 661–669. https://doi.org/10.1634/stemcells.21-6-661

Singh, V., Ulasov, I., Gupta, S., Singh, A., Roy, V. K., & Kharwar, R. K. (2024). Idiopathic Pulmonary Fibrosis: Where do We Stand and How Far to Go? *Discovery Medicine*, *36*(180), 22. https://doi.org/10.24976/Discov.Med.202436180.3

Su, J., Song, Y., Zhu, Z., Huang, X., Fan, J., Qiao, J., & Mao, F. (2024). Cell-cell communication: new insights and clinical implications. *Signal Transduction and Targeted Therapy*, *9*(1), 196. https://doi.org/10.1038/s41392-024-01888-z

Szabó, R., Láng, O., Láng, J., Illyés, E., Kőhidai, L., & Hudecz, F. (2015). Effect of SXWS/WSXWS peptides on chemotaxis and adhesion of the macrophage-like cell line J774. *Journal of Molecular Recognition*, *28*(4), 253–260. https://doi.org/10.1002/jmr.2439

Taga, T., & Kishimoto, T. (1997). <scp>gp</scp> 130 AND THE INTERLEUKIN-6 FAMILY OF CYTOKINES. *Annual Review of Immunology*, *15*(1), 797–819. https://doi.org/10.1146/annurev.immunol.15.1.797

Tai, Y., Woods, E. L., Dally, J., Kong, D., Steadman, R., Moseley, R., & Midgley, A. C. (2021). Myofibroblasts: Function, Formation, and Scope of Molecular Therapies for Skin Fibrosis. *Biomolecules*, *11*(8), 1095. https://doi.org/10.3390/biom11081095

Tan, E., Chin, C. S. H., Lim, Z. F. S., & Ng, S. K. (2021). HEK293 Cell Line as a Platform to Produce Recombinant Proteins and Viral Vectors. *Frontiers in Bioengineering and Biotechnology*, *9*. https://doi.org/10.3389/fbioe.2021.796991

Tang, W., Geba, G. P., Zheng, T., Ray, P., Homer, R. J., Kuhn, C., Flavell, R. A., & Elias, J. A. (1996). Targeted expression of IL-11 in the murine airway causes lymphocytic inflammation, bronchial remodeling, and airways obstruction. *Journal of Clinical Investigation*, *98*(12), 2845–2853. https://doi.org/10.1172/JCI119113

Tenney, R., Stansfield, K., & Pekala, P. H. (2005). Interleukin 11 signaling in 3T3-L1 adipocytes. *Journal of Cellular Physiology*, *202*(1), 160–166. https://doi.org/10.1002/jcp.20100

Torre, A., Martínez-Sánchez, F. D., Narvaez-Chávez, S. M., Herrera-Islas, M. A., Aguilar-Salinas, C. A., & Córdova-Gallardo, J. (2024). Pirfenidone use in fibrotic diseases: What do we know so far? *Immunity, Inflammation and Disease*, *12*(7). https://doi.org/10.1002/iid3.1335

Tsukui, T., Sun, K.-H., Wetter, J. B., Wilson-Kanamori, J. R., Hazelwood, L. A., Henderson, N. C., Adams, T. S., Schupp, J. C., Poli, S. D., Rosas, I. O., Kaminski, N., Matthay, M. A., Wolters, P. J., & Sheppard, D. (2020). Collagen-producing lung cell atlas identifies multiple subsets with distinct localization and relevance to fibrosis. *Nature Communications*, *11*(1), 1920. https://doi.org/10.1038/s41467-020-15647-5

Watsky, M. A., Weber, K. T., Sun, Y., & Postlethwaite, A. (2010). *New Insights into the Mechanism of Fibroblast to Myofibroblast Transformation and Associated Pathologies* (pp. 165–192). https://doi.org/10.1016/S1937-6448(10)82004-0

Widjaja, A. A., Lim, W.-W., Viswanathan, S., Chothani, S., Corden, B., Dasan, C. M., Goh, J. W. T., Lim, R., Singh, B. K., Tan, J., Pua, C. J., Lim, S. Y., Adami, E., Schafer, S., George, B. L., Sweeney, M., Xie, C., Tripathi, M., Sims, N. A., … Cook, S. A. (2024). Inhibition of IL-11 signalling extends mammalian healthspan and lifespan. *Nature*, *632*(8023), 157–165. https://doi.org/10.1038/s41586-024-07701-9

Widjaja, A. A., Singh, B. K., Adami, E., Viswanathan, S., Dong, J., D'Agostino, G. A., Ng, B., Lim, W. W., Tan, J., Paleja, B. S., Tripathi, M., Lim, S. Y., Shekeran, S. G., Chothani, S. P., Rabes, A., Sombetzki, M., Bruinstroop, E., Min, L. P., Sinha, R. A., … Cook, S. A. (2019). Inhibiting Interleukin 11 Signaling Reduces Hepatocyte Death and Liver Fibrosis, Inflammation, and Steatosis in Mouse Models of Nonalcoholic Steatohepatitis. *Gastroenterology*, *157*(3), 777-792.e14. https://doi.org/10.1053/j.gastro.2019.05.002

Widjaja, A. A., Viswanathan, S., Jinrui, D., Singh, B. K., Tan, J., Wei Ting, J. G., Lamb, D., Shekeran, S. G., George, B. L., Schafer, S., Carling, D., Adami, E., & Cook, S. A. (2021). Molecular Dissection of Pro-Fibrotic IL11 Signaling in Cardiac and Pulmonary Fibroblasts. *Frontiers in Molecular Biosciences*, *8*. https://doi.org/10.3389/fmolb.2021.740650

Wilson, M. S., & Wynn, T. A. (2009). Pulmonary fibrosis: pathogenesis, etiology and regulation. *Mucosal Immunology*, *2*(2), 103–121. https://doi.org/10.1038/mi.2008.85

Xu, Y., Kershaw, N. J., Luo, C. S., Soo, P., Pocock, M. J., Czabotar, P. E., Hilton, D. J., Nicola, N. A., Garrett, T. P. J., & Zhang, J.-G. (2010). Crystal Structure of the Entire Ectodomain of gp130. *Journal of Biological Chemistry*, *285*(28), 21214–21218. https://doi.org/10.1074/jbc.C110.129502

Zhang, J.-M., & An, J. (2007). Cytokines, Inflammation, and Pain. *International Anesthesiology Clinics*, *45*(2), 27–37. https://doi.org/10.1097/AIA.0b013e318034194e

Zhou, J., An, X., Xia, X., Xiao, W., Dou, D., Li, W., & Huang, Q. (2025). Aging-associated interleukin-11 drives the molecular mechanism and targeted therapy of idiopathic pulmonary fibrosis. *European Journal of Medical Research*, *30*(1), 542. https://doi.org/10.1186/s40001-025-02755-5

Zhou, Y., Zhang, Y., Zhang, Z., Zhou, Z., & Zhu, F. (2024). AI comes to the Nobel Prize and drug discovery. *Journal of Pharmaceutical Analysis*, *14*(11), 101160. https://doi.org/10.1016/j.jpha.2024.101160